NASA/TM–2020-220437

An Experimental Approach to a Rapid Propulsion and Aeronautics Concepts Testbed

Robert G. McSwain and Steven C. Geuther
Langley Research Center, Hampton, Virginia

Gregory Howland
Analytical Mechanics Associates, Hampton, Virginia

Michael D. Patterson, Siena K. Whiteside and David D. North
Langley Research Center, Hampton, Virginia

January 2020

NASA STI Program . . . in Profile

Since its founding, NASA has been dedicated to the advancement of aeronautics and space science. The NASA scientific and technical information (STI) program plays a key part in helping NASA maintain this important role.

The NASA STI program operates under the auspices of the Agency Chief Information Officer. It collects, organizes, provides for archiving, and disseminates NASA's STI. The NASA STI program provides access to the NTRS Registered and its public interface, the NASA Technical Reports Server, thus providing one of the largest collections of aeronautical and space science STI in the world. Results are published in both non-NASA channels and by NASA in the NASA STI Report Series, which includes the following report types:

- TECHNICAL PUBLICATION. Reports of completed research or a major significant phase of research that present the results of NASA Programs and include extensive data or theoretical analysis. Includes compilations of significant scientific and technical data and information deemed to be of continuing reference value. NASA counter-part of peer-reviewed formal professional papers but has less stringent limitations on manuscript length and extent of graphic presentations.

- TECHNICAL MEMORANDUM. Scientific and technical findings that are preliminary or of specialized interest, e.g., quick release reports, working papers, and bibliographies that contain minimal annotation. Does not contain extensive analysis.

- CONTRACTOR REPORT. Scientific and technical findings by NASA-sponsored contractors and grantees.

- CONFERENCE PUBLICATION. Collected papers from scientific and technical conferences, symposia, seminars, or other meetings sponsored or co-sponsored by NASA.

- SPECIAL PUBLICATION. Scientific, technical, or historical information from NASA programs, projects, and missions, often concerned with subjects having substantial public interest.

- TECHNICAL TRANSLATION. English-language translations of foreign scientific and technical material pertinent to NASA's mission.

Specialized services also include organizing and publishing research results, distributing specialized research announcements and feeds, providing information desk and personal search support, and enabling data exchange services.

For more information about the NASA STI program, see the following:

- Access the NASA STI program home page at http://www.sti.nasa.gov

- E-mail your question to help@sti.nasa.gov

- Phone the NASA STI Information Desk at 757-864-9658

- Write to:
  NASA STI Information Desk
  Mail Stop 148
  NASA Langley Research Center
  Hampton, VA 23681-2199

NASA/TM–2020-220437

An Experimental Approach to a Rapid Propulsion and Aeronautics Concepts Testbed

Robert G. McSwain and Steven C. Geuther
Langley Research Center, Hampton, Virginia

Gregory Howland
Analytical Mechanics Associates, Hampton, Virginia

Michael D. Patterson, Siena K. Whiteside and David D. North
Langley Research Center, Hampton, Virginia

National Aeronautics and
Space Administration

Langley Research Center
Hampton, Virginia 23681-2199

January 2020

Available from:

NASA STI Program / Mail Stop 148
NASA Langley Research Center
Hampton, VA 23681-2199
Fax: 757-864-6500

Abstract

Modern aircraft design tools have limitations for predicting complex propulsion-airframe interactions. The demand for new tools and methods addressing these limitations is high based on the many recent Distributed Electric Propulsion (DEP) Vertical Take-Off and Landing (VTOL) concepts being developed for Urban Air Mobility (UAM) markets. We propose that low cost electronics and additive manufacturing can support the conceptual design of advanced autonomy-enabled concepts, by facilitating rapid prototyping for experimentally driven design cycles. This approach has the potential to reduce complex aircraft concept development costs, minimize unique risks associated with the conceptual design, and shorten development schedule by enabling the determination of many "unknown unknowns" earlier in the design process and providing verification of the results from aircraft design tools. A modular testbed was designed and built to evaluate this rapid design-build-test approach and to support aeronautics and autonomy research targeting UAM applications utilizing a complex, transitioning-VTOL aircraft configuration. The testbed is a modular wind tunnel and flight model. The testbed airframe is approximately 80% printed, with labor required for assembly. This paper describes the design process, fabrication process, ground testing, and initial wind tunnel structural and thermal loading of a proof-of-concept aircraft, the Langley Aerodrome 8 (LA-8).

Contents

Nomenclature 1
Introduction 2
RapidPACT Team 3
Approach 4
Conceptual Design 5
Mechanical Design and Fabrication 18
Electronics Design and Fabrication 29
Ground Testing 43
Lessons Learned 53
Future Work 54
References 54

List of Figures

Figure 1. RapidPACT Milestone Overview 4
Figure 2. Vertical Flight Society Wheel of Fortune (Ref. 4) 6
Figure 3. NASA GL-10 50% Scale Flight Demonstrator 7
Figure 4. Ryan VZ-3 at U.S. Army Aviation Museum's Showroom 7
Figure 5. Initial LA-8 Conceptual Design 9
Figure 6. Final LA-8 Vehicle Design 10
Figure 7. Front View of LA-8 Showing Propeller Rotation Assignment 12
Figure 8. LA-8 Top View Actuator/Effector Map (surface sizes not to scale) 15
Figure 9. LA-8 XFLR5 Lifting Surface Geometry 16
Figure 10. LA-8 Power-Off L/D Estimates for Various Airspeeds 16
Figure 11. LA-8 XFLR5 Estimation for Aerodynamic Coefficients vs. Angle of Attack (lower figures) and Sideslip Angle (upper figures) 17
Figure 12. Brass Insert Embedded Into Nylon 18
Figure 13. LA-8 Fuselage Test Parts 19
Figure 14. FDM Nylon 12 Fuselage Section 20
Figure 15. Onyx Winglet 20
Figure 16. PC Access Hatch 21
Figure 17. LA-8 Fuselage Sections 22
Figure 18. LA-8 Fuselage Cooling Inlet Ducts 22
Figure 19. Forward and Aft Wing Sections 24
Figure 20. LA-8 Airfoil Prototype Test Part 24
Figure 21. Nacelle Attachment Prototype 25
Figure 22. Foam Core Carbon Fiber Forward Wing Load Test Article 26
Figure 23. LA-8 Wing Actuator Design 28
Figure 24. LA-8 Wing Actuator 28
Figure 25. LA-7 Control Architecture 29
Figure 26. LA-7 CERTAIN Net Hover Flight Testing 31
Figure 27. LA-7 CERTAIN Transition Flight Testing 31
Figure 28. Control System Architecture 32
Figure 29. Data System Architecture 34

Figure 30. Custom Low Cost Air Data Probe....34
Figure 31. Low-Cost/High Angle Alpha/Beta Probe....35
Figure 32. Analog Input Nomenclature Assignments....36
Figure 33. Power System Architecture....37
Figure 34. Electronic System CAD Model....38
Figure 35. LA-8 Electronics Upper Tray Assembly....38
Figure 36. LA-8 Electronics Lower Tray Assembly....39
Figure 37. Upper and Lower Trays Located in the Fuselage....40
Figure 38. LA-8 Upper and Lower Tray w/Harnesses....41
Figure 39. Electronics and Mechanical Integration Fit Test....42
Figure 40. 21.5x7.5 inch 3 Bladed Propeller Static Thrust Data....43
Figure 41. 16x8 inch 3 Bladed Propeller Static Thrust Data....44
Figure 42. Wing Actuator Moment Test Setup....45
Figure 43. Drive Assembly Driven @ 8.0V....46
Figure 44. Control, Power and Auxiliary Systems Ground Test Setup....47
Figure 45. LA-8 Control Surface and Motor Ground Test....47
Figure 46. LA-8 65lb 3G Load Test....48
Figure 47. LA-8 Secured During Thermal Testing....49
Figure 48. Diode Test Abort Temperature @ 72lb Total Thrust....50
Figure 49. Steady State ESC Temperature @ 64lb Total System Thrust....51
Figure 50. Internal ESC Temperature @ 64lb Total System Thrust....51
Figure 51. ESC Temperature @ 64lb Total System Thrust w/Cooling Fans....52
Figure 52. Steady State Motor Temperature @ 64lb Total System Thrust....52

List of Tables

Table 1. LA-7 Specifications....30
Table 2. LA-8 Flight Controller Output Assignments....33

Nomenclature

ARMD = Aeronautics Research Mission Directorate
CAN = Controller Area Network
CAS = Convergent Aeronautics Solutions
CERTAIN = City Environment for Range Testing of Autonomous Integrated Navigation
CFD = Computational Fluid Dynamics
DELIVER = Design Environment for Novel Vertical Lift Vehicles
DEP = Distributed Electric Propulsion
DOE = Design of Experiment
GL-10 = Greased Lightning
I2C = Inter-Integrated Circuit
L2F = Learn to Fly
LA-7 = Langley Aerodrome 7
LA-8 = Langley Aerodrome 8
LaRC = Langley Research Center
MTOW = Maximum Takeoff Weight
MUX = Multiplexer
NAS = National Airspace System
ODM = On-Demand Mobility
OML=Outer Mold Line
PCB = Printed Circuit Board
PID= Proportional-Integral-Derivative
PWM = Pulse Width Modulation
RapidPACT = Rapid Propulsion and Aeronautics Concepts Testbed
RC = Remote Control
SBC = Single Board Computer
SIP = Strategic Implementation Plan
SPI = Serial Peripheral Interface
sUAS = small Unmanned Aircraft Systems
TACP = Transformative Aeronautics Concepts Program
TTT = Transformational Tools and Technologies
UAM = Urban Air Mobility
VTOL = Vertical Take-Off and Landing

$C_{\ell,\beta}$ = Change in aircraft rolling moment coefficient with respect to sideslip angle
$C_{m,\alpha}$ = Change in aircraft pitching moment coefficient with respect to angle of attack
$C_{n,\beta}$ = Change in aircraft yawing moment coefficient with respect to sideslip angle

Introduction

The RapidPACT project was focused on improving the systems engineering and analysis tools used for early stage concept development of vehicles, where physical system-level data may be unavailable. The use of physical modeling is not typical in the early design phases because of the long cycle time and high cost of wind tunnel testing and flight model production, and conceptual design models are typically limited in their ability to model novel configurations, such as those with complex aeropropulsive interactions. CFD and other computer-based performance analysis tools are often used to make assessments of new design concepts with high-cost physical models constructed and tested to validate the computer modeling. However, new flight vehicle concepts that have complex flow from multiple propulsion units and non-traditional airframe designs are difficult to analyze with traditional conceptual design methods due to a lack of historical data for comparison. In addition, high fidelity CFD can be computationally time consuming even for relatively simple configurations. With the advent of new rapid prototyping and analysis techniques, we propose to design, build and test new concepts in a short time frame in order to influence choices made in the early stages of the design cycle and to provide calibration data for analysis tools for future designs. This method will enable more insight into the vehicle design early in the process and could lower risk by preventing system-level design oversights that are often extremely costly or irreversible in the late stages of a design. For example, risks associated with control and stability during transition, due to aeropropulsive interactions and high lift devices, could be mitigated by this method.

During fiscal year 2018, the RapidPACT project was focused on developing the processes, tools and methods for rapid prototyping. NASA Langley Research Center has experience from recent flight projects (e.g. L2F (Ref. 1) and DELIVER (Ref. 2)) researching and developing advanced aeronautics concepts. This experience provides an opportunity for comparison of new tools and methods developed. This report documents the design, fabrication and testing of a generic UAM research testbed. The work has transitioned into the NASA TTT project in fiscal year 2019 to validate new prediction tools and methods through wind tunnel testing.

RapidPACT Team

Principle Investigator - David North
Project Manager - Robert McSwain

Aircraft Conceptual Design

Steven Geuther
Michael Patterson
Xiaofan Fei
Siena Whiteside

Model Design and Fabrication

Greg Howland
Christopher Cagle
David Bradley
Jared Fell

Electronics and Data System

Neil Coffey
David Hare
Toby Comeaux
Justin Lisee
William Chambers

Approach

Because the project proposed building physical wind tunnel and flight models, an interdisciplinary team was needed. This enabled our team to have a broad range of experience that is critical for developing highly integrated prototypes. Agile project management principles were utilized to facilitate the interdisciplinary approach. The principles that the team valued included: Individuals and Interactions over processes and tools; Working Software/Hardware over comprehensive documentation; Customer Collaboration over defining requirements; Responding to Change over following a plan (Ref. 3). Value was placed on utilizing scalable and reproducible design and manufacturing methodologies. Parts/components with complex surface geometry were targeted for 3D printing while internal structures were targeted for commercially available materials. Low cost electronic components that were readily available from vendors were used. All of this was intended to enable the design, build and testing of wind tunnel and flight model faster and at lower cost than traditional machining and/or carbon lay-up. Our proposed approach would provide great value for early conceptual design where parameter trends are more useful than exact values to inform major configuration design decisions. Our proposed work included a flight test and wind tunnel test in a two year period of time with an objective to provide an order of magnitude reduction in cost compared to existing methods. Figure 1 shows the project milestones and their associated schedule dates. The light green markers indicate completed milestones and milestones beyond the work covered in this report are colored red.

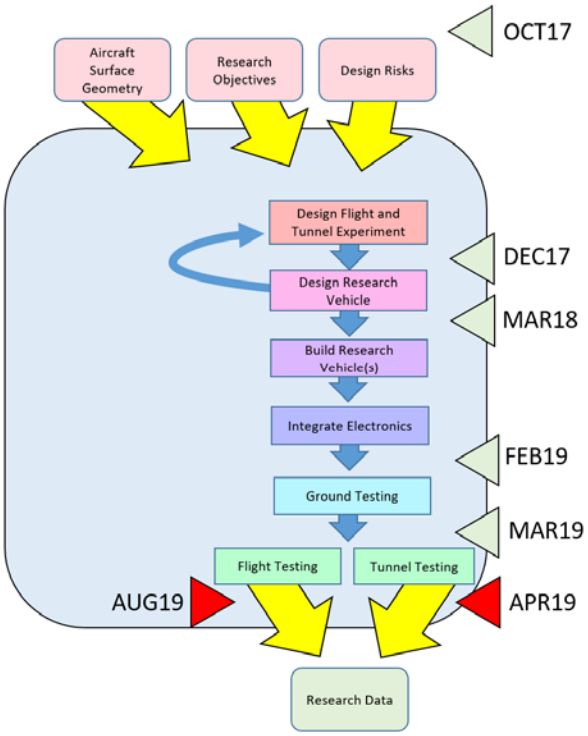

Figure 1. RapidPACT Milestone Overview

Conceptual Design

In order to start the RapidPACT process, a conceptual design was required to prototype and test. The project was asked to utilize a UAM aircraft concept to initiate the rapid prototyping process. Inspiration was taken from Figure 2 (Ref. 4), as well as past and current projects. Some of the other projects that were taken into consideration were the NASA GL-10, Ryan VZ-3, Airbus Vahana, Zee Aero Z-P2, and the Aurora XV-24 Lightning Strike. The objectives of the conceptual design process were to design a vehicle that would possess potentially very high performance while also having several high-risks aspects. The intent was that through the rapid design process the technical risks to the vehicle would be both articulated, managed, and a point of focus for early retirement. The resulting design features potentially high performance as a result of its ability to achieve wing-borne forward flight with folding props and relatively high wing-loading. The vehicle's VTOL capabilities would address requirements for UAM operations at vertiports in urban areas.

The risks identified for this design concept are:

1) Adequate control power for transition.
2) Stability of the vehicle in transition and forward flight.
3) Effects of distributed electric propulsion on vehicle stability and control.
4) Aeroperformance metrics for cruise (ie L/D).
5) Engine failure for hover, transition, and forward flight and back to hover for landing.
6) Effect of oversized flaps and DEP to minimize wing angle tilting during transition.
7) Control failure for hover, transition, and forward flight and back to hover for landing.
8) Effects of winds on vehicle handling and control in hover and transition.
9) Limited payload due to vertical lift requirements combined with control system margin.

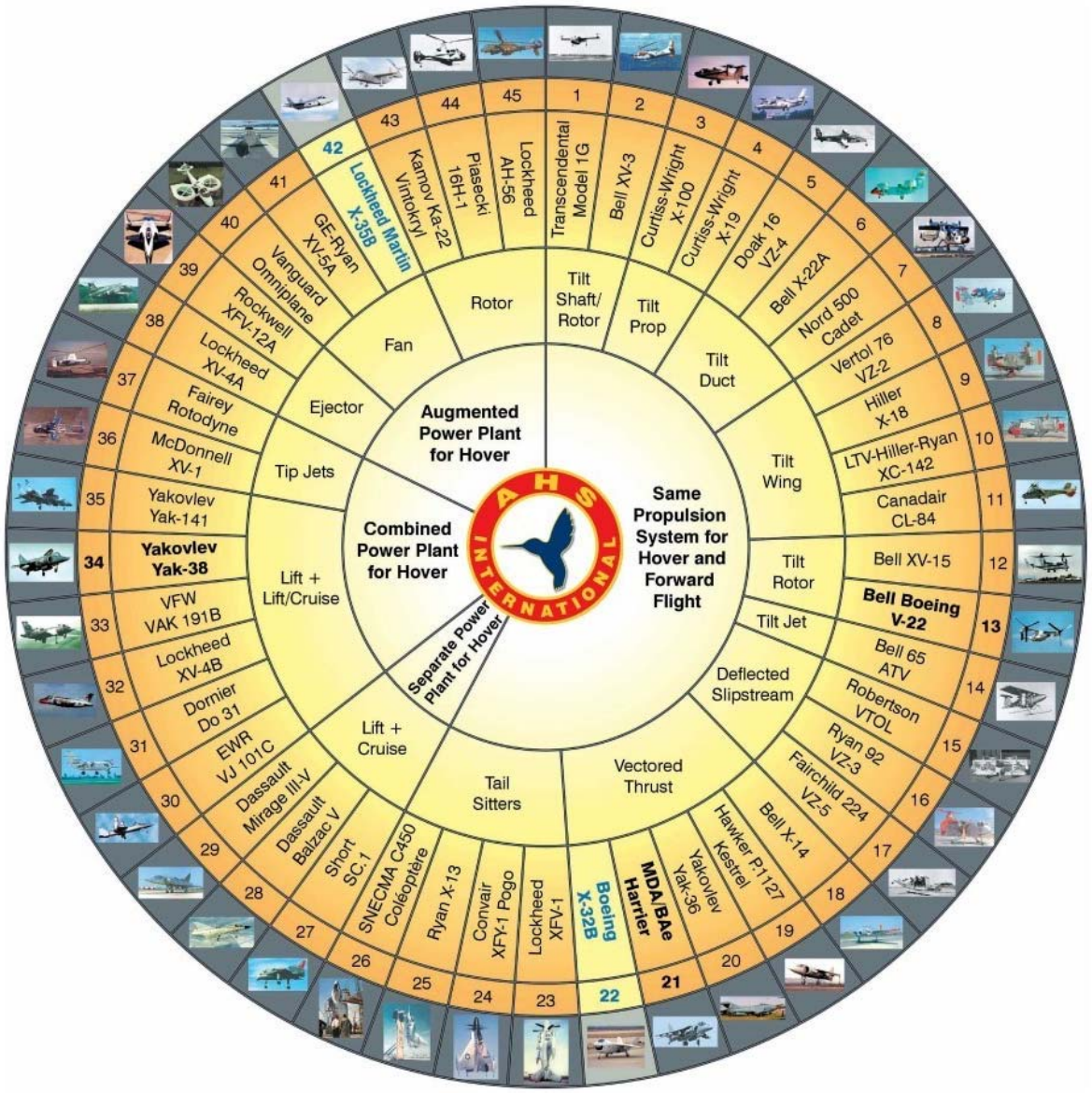

Figure 2. Vertical Flight Society Wheel of Fortune (Ref. 4)

When starting the first design iteration, the Aircraft Conceptual Design Team began with the basic mission, vehicle requirements, and modeling/testing constraints. The main goal was to design a VTOL aircraft applicable to a UAM mission. This concept would have a maximum wingspan of 8 ft (to include wingtip propellers) in order to allow prediction tools to be validated against experiments in the NASA LaRC 12 ft Low Speed Wind Tunnel. It was also desired to develop a single prototype that could be tested both in a wind tunnel and outdoors to accelerate the testing timeline. For practical implementation, an all-electric propulsion system was to be used. It was also desired that the aircraft could be controlled manually at small test ranges and be statically stable in case of power loss. Finally, it was highly desirable that the final design be able to utilize the same propellers employed on the GL-10 aircraft, which were 16 inch diameter, 8

inch pitch, three-bladed propellers, in order to reduce costs and timeline risk from needing to procure and characterize new propellers. These design requirements provided the foundation for a vehicle concept to be designed.

The Aircraft Conceptual Design Team had multiple design brainstorming sessions to propose new configuration concepts and used OpenVSP (Ref. 5) for the modeling of configurations as a visual aid in configuration design discussions. In addition to these concepts, the team discussed how new technologies may be used to improve upon previous concepts. Eventually, after considering many different concepts, the team decided on a DEP tandem tilt-wing configuration that combines elements of the NASA GL-10, pictured in Figure 3, and the Ryan VZ-3 Vertiplane, pictured in Figure 4.

Figure 3. NASA GL-10 50% Scale Flight Demonstrator

Figure 4. Ryan VZ-3 at U.S. Army Aviation Museum's Showroom

The GL-10 utilized a tilting wing and a tilting, lifting tail along with DEP for VTOL operations. One of the difficulties with tiltwing vehicles is the flow separation that occurs at high wing incidence angles in transition from vertical to horizontal flight (and back) when the wing experiences high angles of attack and low forward flight speeds. In the high wing incidence angle portion of the transition corridor, tiltwing aircraft can experience buffeting and other adverse characteristics, such as a loss of altitude or a loss of control power. The DEP system on

the GL-10 delayed stall over a large portion of the wing through the transition corridor, but some flow separation issues were still present. Furthermore, when in vertical flight mode, tiltwing aircraft have large frontal areas which make them susceptible to gusts. The Aircraft Conceptual Design Team considered potential solutions in which these shortcomings could be addressed, which led them to explore deflected slipstream aircraft, such as the Ryan VZ-3.

The VZ-3 relied on deflecting the slipstream from two large propellers downward via a flap system to achieve very high lift at zero forward flight speed. Deflected slipsteam concepts like the VZ-3 have the potential to mitigate some of the high angle of attack problems experienced by tiltwings in the transition corridor because the wing is not tilted to a very high incidence angle. [1] However, the VZ-3 experienced issues when attempting VTOL flight, including pitch instabilities and propellers losing thrust/efficiency from reingesting their own silpstreams that deflected off of the ground plane (Ref. 6). The conceptual design team hypothesized that a deflected slipstream concept with DEP could potentially overcome these issues. By distributing the propulsion across multiple wings or a wing and a tail, as was done on the GL-10, the pitch stability issues of a deflected slipstream concept may be mitigated. Additionally, by spreading out the flow over a larger number of propellers than the original VZ-3 aircraft, less mass flow of air would be present at any single location, which could reduce the potential problems of flow reinjestion from propeller slipstreams deflecting off of the ground and causing thrust/efficiency loss problems. However, deflected silpstream concepts will inevitably incur some losses as the flow from the propellers is turned by the wing and flap system through approximately 90 degrees, which can lead to increased power requirement for vertical flight compared to a tiltwing concept.

In an attempt to balance the advantages and disadvantages of the deflected slipstream and tiltwing vehicle concepts, the Aircraft Conceptual Design Team developed a notional combined tandem tiltwing-deflected slipstream vehicle. In this concept, there are three separate mechanisms that can be combined to achieve a vertical resultant force: the wing (and therefore propeller) incidence angle relative to the fuselage, the flap design and deflection angle, and the fuselage angle relative to the ground set by the landing gear. This aircraft would achieve vertical flight by fixing the wings at an intermediate incidence angle (i.e., at an angle between the near-zero degree angle of a deflected slipstream concept and the near-90 degree angle of the tiltwing) and would rely on a flap system to deflect the propeller slipstreams to achieve a resultant force solely in the vertical direction. From an efficiency perspective, there are advantages to having minimal flow turning from the flap to reduce turning losses; therefore, a higher wing incidence angle relative to the ground is desired at takeoff. However, traditional airplane's wing incidence angles are only a few degrees in order to achieve low cruise drag from the fuselage. In order to achieve a relatively high wing incidence angle relative to the ground without requiring a large incidence angle relative to the fuselage, a non-traditional landing gear design can be utilized that elevates the nose of the aircraft for VTOL operations. A detailed conceptual design study could

[1] In deflected slipstream concepts, flap elements are tilted through large angles, but the main wing element does not tilt.

weigh the tradeoffs within the design space for this concept to achieve a high-performing aircraft design.

One of the purposes of the RapidPACT project was to demonstrate a rapid prototyping technique and testing process that would inform subsequent iterations of an aircraft design. Therefore, a rapidly designed, versatile version of the combined tiltwing-deflected slipstream aircraft was selected for the first iteration of the RapidPACT vehicle, which was named Langley Aerodrome 8 (LA-8).[2] An existing airfoil and flap design was utilized and the wings were given the ability to rotate up to 90 degrees to test different wing incidence angles relative to the fuselage. The first conceptual design cycle, including definition of the concepts of operation and outer mold line (OML), was completed in approximately 1 to 2 months. [3] This OML is shown in Figure 5 and was provided to the Model Design and Fabrication Team for the mechanical design and manufacturing of a physical test model. During this process, discussions among RapidPACT team members led to several changes to the OML by both the Aircraft Conceptual Design Team and the Model Design and Fabrication Team, and the resulting final OML is shown in Figure 6.

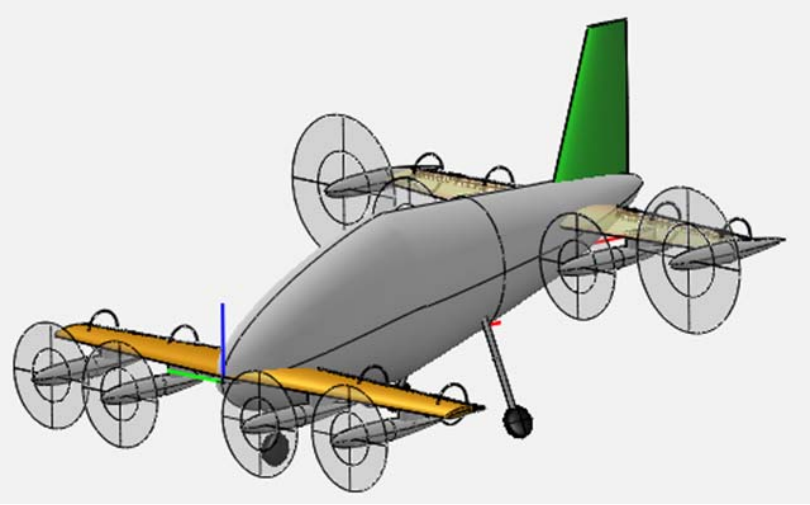

Figure 5. Initial LA-8 Conceptual Design

[2] This name is based on the previous series of tandem wing "aerodrome" aircraft that Samuel P. Langley, the man for whom NASA Langley Research Center is named, built in the 1890s and early 1900s.

[3] It should be noted that no member of the RapidPACT team was working full time on the project. It is likely that the actual work occurred in a matter of a few weeks.

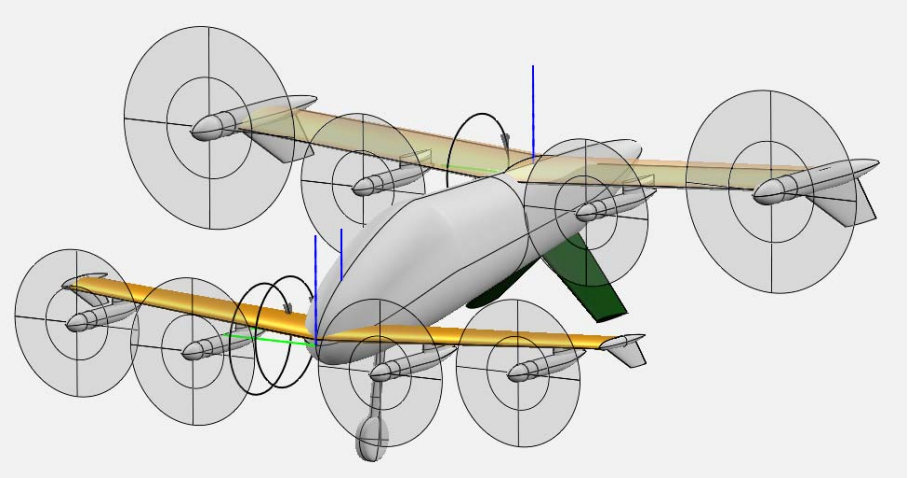

Figure 6. Final LA-8 Vehicle Design

Based on inputs from the Model Design and Fabrication Team as well as considering existing regulations, a 55 lb gross weight was used for all calculations during the design phase. This would allow the aircraft to be operated as a small sUAS under 14 CFR § 107.

The fuselage of the aircraft was desired to be as small as practical to reduce drag while still maintaining a sufficient internal volume for instrumentation and other payload, including the ability to adjust the center of gravity location. The center of gravity adjustments were particularly important to consider in the design process because the fuselage was also designed in a modular fashion so that different wing sets could be attached to it. To increase the aerodynamic efficiency of the configuration, the fuselage was designed to accommodate wings that are offset vertically to minimize interactions between the wake of the front wing, the aft wing and propellers. However, this vertical wing offset creates an upward taper of the fuselage, which creates some concerns with regards to formation of an adverse pressure region on the bottom surface. To reduce the likelihood of this taper causing additional drag, the fuselage taper angle was set to a relatively low value. Future testing will determine if flow separation occurs and creates any issues for the aircraft in the operating airspeed range.

In order to facilitate rapid prototyping of the test vehicle, the decision on the number of rotors was determined based on the size of the GL-10 folding propellers, which were available and had previously been tested in a wind tunnel. Utilizing the GL-10 propellers and the span constraints for entry into the wind tunnel, a maximum of eight non-overlapping propellers could be used; consequently, the vehicle was designed with eight propellers in order to achieve maximum disk area and blown wingspan. Having the propellers blow as much of the span as possible reduces the percentage of stalled airfoil sections over the tilting wing in transition and increases the lift generated from the wing in low speed forward flight and vertical flight.

Additionally, the team decided to place propellers at the wingtips of the aft wing to reduce drag in forward flight. Wind tunnel testing (Ref. 7) as well as theoretical and computational studies (Ref. 8, 9) have demonstrated that spinning propellers at the wingtips counter to the wingtip vortex provides a beneficial aeropropulsive coupling that reduces induced

drag. The inclusion of wingtip propellers was considered important for this particular configuration because the 8 ft maximum span constraint led the wings to be fairly low aspect ratio, and the beneficial tip propeller effects has the ability to offset some of the increased induced drag from the relatively high span loading. In order to achieve as high of a wing aspect ratio and have the tip propellers blow as much of the span as possible, the wingtip propellers on the aft wing were increased to a 22 in diameter. Because these wingtip propellers would be operated throughout all phases of flight, there was no requirement for the blades to fold, which allowed multiple options for selecting commercial off the shelf wingtip propellers.

With six 16 inch diameter propellers and two 22 inch diameter propellers, the disk loading was determined to be 4 lb/ft^2, which is approximately equivalent to the GL-10. In addition, because GL-10 propellers can fold, only the two larger wingtip propellers would be utilized during forward flight while all eight propellers would be powered for vertical flight, hover, and transition.

The placement of the six folding propellers was another important design consideration. These propellers were placed below the wing chord line based on lessons learned through the design process of the X-57 and design guidelines from past deflected slipstream and externally blown flap configurations (Refs. 10, 11). Specifically, if the nacelles are integrated into the wing directly, the suction peak of the airfoil can be significantly reduced as the airfoil geometry is modified to account for a smooth integration of the nacelle. This reduction in the airfoil suction peak can cause a substantial loss in lift, which is detrimental for transition characteristics and the effectiveness of the deflected slipstream concept. Furthermore, because the LA-8 will employ flaps, placing the propellers below the wing chord line enables an externally blown flap geometry, which can increase the lift generated from the wing and effectively deflect the propeller slipstreams downward. The propeller disc planes were placed one radius ahead of the leading edge of the wing to allow for folding.

The LA-8 was designed to have all the propellers rotate in the direction opposite to the wingtip vortices relative to the symmetry plane because such rotation directions have been shown to reduce the overall induced drag. By having all propellers on a wing rotate in the same direction, vortex interactions between the propellers are reduced when compared with rotating them in opposite directions, and rotating tip propellers counter to the wingtip vortex can reduce induced drag as was previously described. Therefore, all propellers were selected to rotate in a down outboard direction as shown in Figure 7.

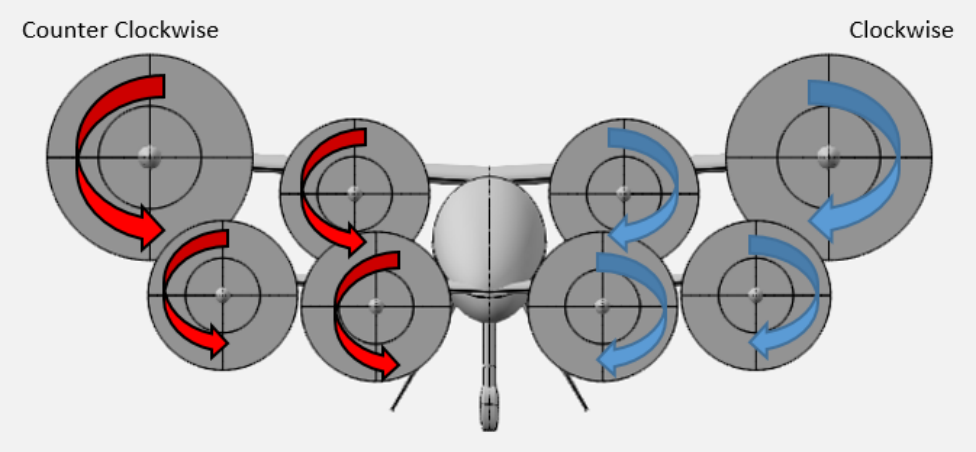

Figure 7. Front View of LA-8 Showing Propeller Rotation Assignment

The next aspect of consideration was the wing design, which started by considering the airfoil. Deflected slipstream concepts rely on non-traditional airfoil and flap designs to effectively turn the propeller slipstreams. Specifically, based upon deflected slipstream research data from Kuhn and Draper (Ref. 12), the C_L and C_D values that are needed for VTOL for deflected slipstream concepts are possible using double slotted flaps. However, to reduce the mechanical complexity of the first design iteration in order to simplify the manfuacturing processes, the RapidPACT team decided that either a plain flap or a single slotted flap should be utilized. Although such a design would not be effective for a full deflected slipstream concept, it can still provide flow turning and relatively high lift characteristics. Insufficient time and resources were available to peform a novel airfoil and flap design for the Reynolds numbers appropriate for LA-8. Therefore, the airfoil was selected as the single slotted flap design from the X-57 project, which is a 25% chord flap (Ref. 13). This airfoil was designed for a higher Reynolds number regime than the LA-8, which is likely to lead to sub-optimal performance, but subsequent design iterations could include a dedicated airfoil and flap design to improve the performance.

The wing planform designs were set through a combination of the propeller selection and maximum dimension constraints from the wind tunnel, as well as consideration of the static longitudinal stability of the aircraft. The front wing span was designed for two propellers to effectively blow all of the wing (outside of the fuselage) in their slipstreams. The aft wing span was set in conjunction with the tip propeller size selection to maximize its span while still ensuring that a large portion of the span was blown by the propeller, as was described previously. The total wing area was set so that the aircraft would have similar wing loading to the GL-10 aircraft, which was approximately 80 oz/ft^2. The distribution of this total wing area between the front and aft wings was an iterative process based on analysis of the longitudinal static stability of the aircraft and by the desire to limit the aspect ratio of the wings to no more than 9.0 and no less than 5.0 to ensure the RapidPACT manufacturing processes could create a sufficiently strong structure, but not increase the induced drag significantly. Both wings are tapered to improve the span loading characteristics. The front wing planform was designed with a 6 inch tip

chord, the minimum value desired for manufacturing considerations, an 11.4 inch root chord, and a 5.8 ft span. The aft wing was designed with a 1.25 ft root chord, a 1.0 ft tip chord, and a 6.2 ft span.

After performing stability analyses, the incidence angles of the wings for forward flight were set to 1.0 degree for the aft wing and 3.5 degrees for the front wing. Since the airfoils are same on both wings, the higher incidence angle of the front wing is beneficial to help ensure that the front wing stalls prior to the aft wing in forward flight conditions. Additionally, a few degrees of dihedral were added to each wing to provide natural stability. Both wings were also designed with 2.0 degrees of washout to provide desireable stall characteristics. These wing features provided additional complexity in manufacturing, which ensured that the experimental prototyping process included considerations for these design options.

The final aspect of the wing design was the addition of wing endplates. Based on previous wind tunnel testing of deflected slipstream concepts, endplates are necessary to allow the wing and flap system to effectively turn the slipstream from the propellers downward (Ref. 6, 12). However, a design for the optimum size and shape of these endplates is currently unknown. The conceptual design team requested that endplates were removable, so that different designs could be evaluated.

In order for the vehicle to be naturally laterally and directionally stable, there was a need for vertical tail surfaces. Although the original conceptual design placed the vertical tail above the fuselage, there were multiple concerns with this placement. In situations where the wing would be at moderate to high incidence angles, such as in transition, a noticable portion of the vertical tail would be blocked by the presence of the wing. In fixed wing flight at high angles of attack, the vertical tail effectivness could be weakened by flow separating from the wing. Also, the rudder would be well above the center of gravity, which would create a noticeable rolling moment in addition to the desired yawing moment with a maximum deflection. To overcome these issues, the single vertical tail was removed in favor of an inverted “V” tail placed on the bottom of the fuselage below the aft wing. This change allowed the surfaces to double as landing gear, which could reduce the overall wetted area of the configuration. The tail surface thicknesses were sized with structural requirements, and NACA 0015 airfoils were selected for these surfaces. The dihedral angle was initially set based on the tip over considerations for the landing gear, and slight modifications to this angle were made as stability analyses were performed so that the aircraft could achieve static lateral and directional stability.

Throughout the design process, an integral aspect was the placement of the center of gravity (CG). As a transitioning VTOL vehicle, there was consideration of both forward and vertical flight modes in the design process. Because the vehicle is a tiltwing with motors and propellers placed well ahead of the wing center of rotation, the aircraft CG shifts forward during the transition from vertical to horizontal flight when the wings tilt downward; therefore, the vehicle has two CG locations based on its mode of operation. Because the aft wing was designed to produce more lift than the front wing in forward flight, the ideal CG placement for cruise is closer to the aft wing than the front wing (with the wings rotated down to their forward flight

incidence angles). However, for vertical flight, an ideal CG location would allow an identical disk loading on each individual propeller, which would place the CG with the wings rotated upward slightly aft of the midpoint between the two wings (because the total propeller disk area is slightly greater on the aft wing than the front wing). If the CG were located at the optimum point for hover power requirements, after the wings tilt downward, the CG would be noticably further forward than would be desired for forward flight. Consequently, the CG location selected for the final design provided a compromise between hover power requirements and natural stability in forward flight. The final CG location was 1.9 ft aft (x-direction) and 0.65 ft up (z-direction) from the nose and along the symmetry plane of the aircraft in forward flight.

The final phase of the design process involved sizing the control surfaces. Prior experience from the GL-10 was considered heavily in the process. Although full-span flaps would have led to improved flow turning for the deflected slipstream portion of the concept, the X-57 flap design would not allow for the flaps to act as practical ailerons or elevators due to the inability to deflect upwards. Consequently, separate elevons were added to the outboard portions of both wings. The elevons were sized at 50% chord length and 35% chord length on the front and aft wings, respectively, to give an approximately equal elevon area on both wings. These fairly large chord lengths were selected based on lessons-learned in the GL-10 flight testing. Specifically, the GL-10 relied on elevon deflections in the propeller slipstreams to control yaw in hover, and the aircraft exhibited less than desirable yaw control authority. Consequently, a large elevon area on the LA-8 was selected to improve the yaw control authority in vertical flight. As a potential additional improvement, the combined deflected slipstream-tiltwing design of the LA-8 may allow differential propeller thrust and elevon/flap deflection to control yaw in hover if the wing angles can be sufficiently below 90 degrees. Overall, there were 20 actuators/control effectors (i.e., motors, elevons, ruddervators, flaps, and wing actuators) designed into the vehicle, 18 of which can be seen in Figure 8. These control surfaces are not drawn to scale. The two control surfaces not shown in the figure are the two ruddervators, which are located on the inverted “V” tail surfaces and were set at 30% chord length.

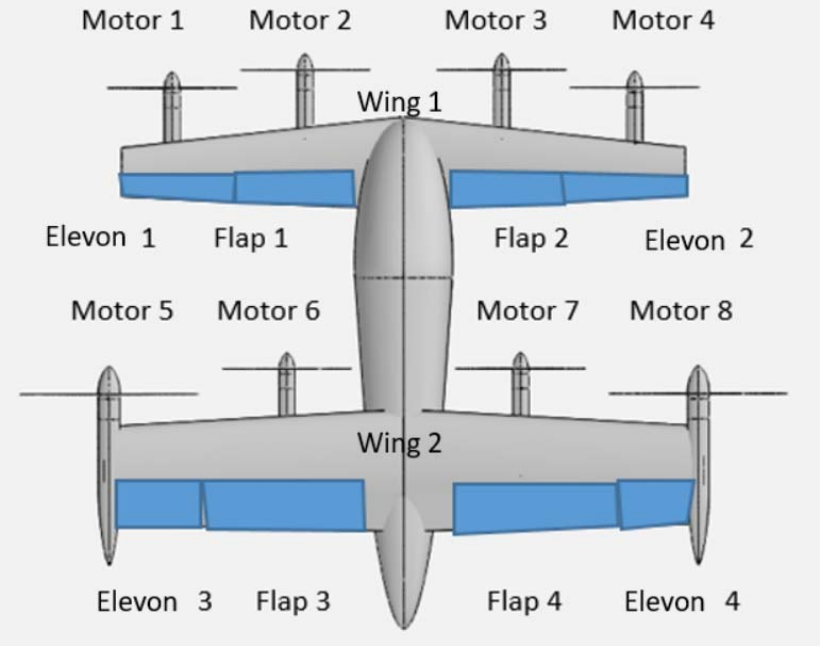

Figure 8. LA-8 Top View Actuator/Effector Map (surface sizes not to scale)

In order to estimate the stability and performance of the aircraft, two computational tools were used. XFLR5 (Ref. 14), a vortex lattice method analysis tool that is inherently coupled with XFOIL (Ref. 15), provided estimates of the lift, static stability, induced drag, and profile drag with a lifting-surface-only geometry, as shown in Figure 9. To estimate the parasitic drag of the aircraft, a component drag buildup method was implemented in a spreadsheet. The drag of each component (e.g., fuselage, main wing, etc.) was first estimated based on the skin friction drag of a flat plate with the same characteristic length as the component. Then this flat plate drag estimate was modifed to approximate the drag of the entire three-dimensional component with a form factor (Ref. 16) based on the component type (e.g., wing, body) and the wetted area of the component, which was estimated with OpenVSP. Finally, interference drag and excrescence drag were accounted for by multiplying the resulting drag of components by correction factors, which were based on general guidelines (Ref. 17) and previous analyses.

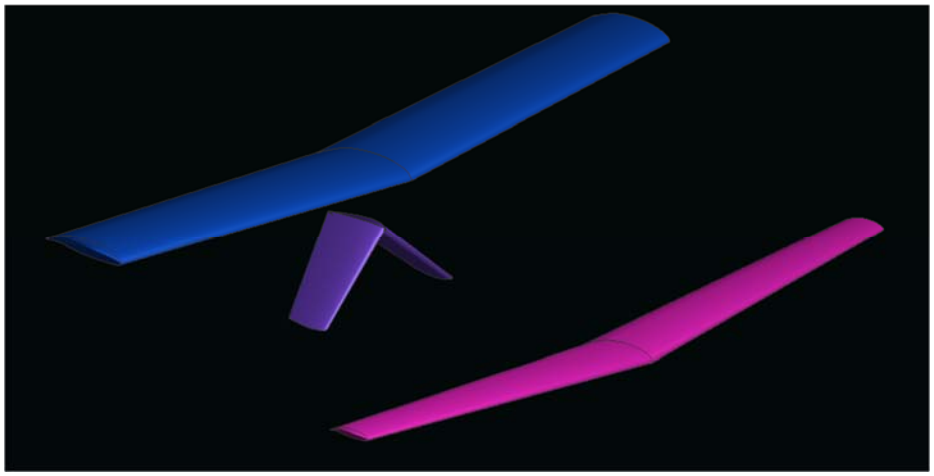

Figure 9. LA-8 XFLR5 Lifting Surface Geometry

The forward flight performance of the aircraft was estimated with the calculated lift and drag values for the aircraft resulting from the XFLR5 and parasite drag analyses. This analysis excludes the impacts of the thrust and slipstreams from the wingtip propellers. Because the center of the wingtip propellers are above the CG, there will be a nosedown pitching moment generated in forward flight, which must be offset for the aircraft to trim. This can be accomplished by adjusting control surfaces, which will increase the drag compared to the predicted value. However, the wingtip propellers should reduce the induced drag. For these initial performance calculations, these competing effects were assumed to negate one another, even though this will not likely be the case in practice. By analyzing different angles of attack, conditions where the lift was equal to the weight were found, and the approximate lift to drag ratio, L/D, was determined over a range of airspeeds. The forward flight L/D values predicted for a range of airspeeds are shown in Figure 10, and the peak cruise L/D was observed at approximately 90 ft/s (53 knots).

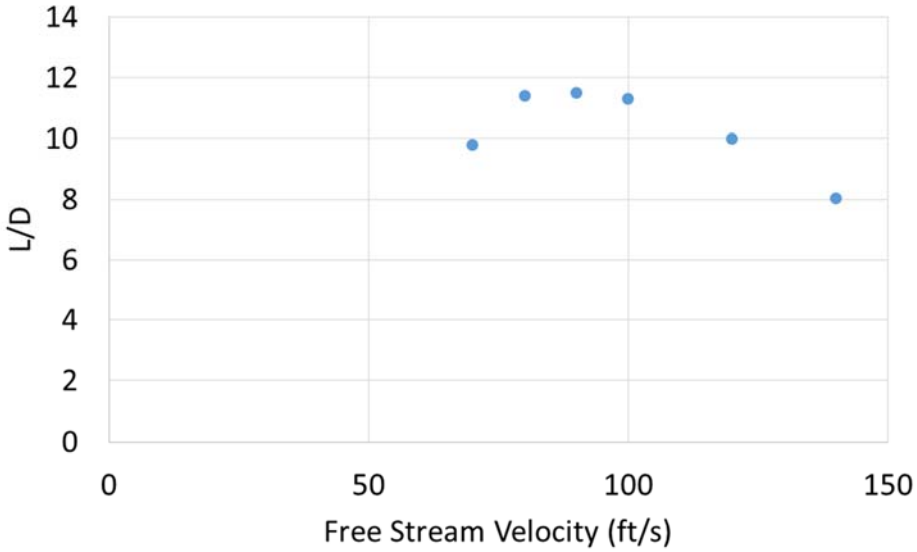

Figure 10. LA-8 Power-Off L/D Estimates for Various Airspeeds

Estimates of the stability derivatives $C_{m,\alpha}$, $C_{\ell,\beta}$, and $C_{n,\beta}$ were made, and these parameters are shown in Figure 11. The results in the figure are only approximate due to the vortex lattice method's inability to consider the impacts of the propellers, fuselage, and nacelles. Thrust effects are likely to cause substantial changes in these parameters; however, this analysis indicates that the aircraft should be statically stable in power-off conditions.

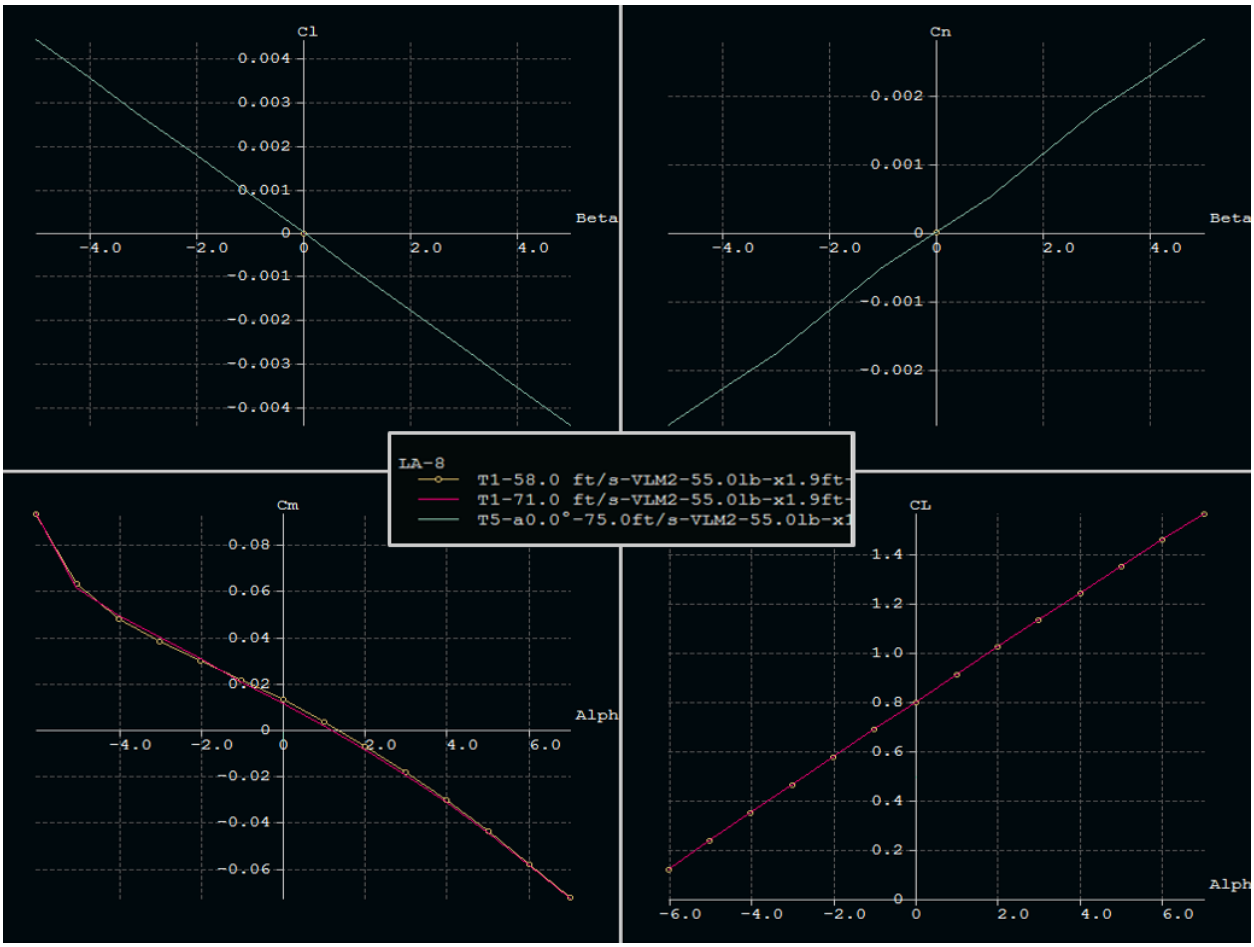

Figure 11. LA-8 XFLR5 Estimation for Aerodynamic Coefficients vs. Angle of Attack (lower figures) and Sideslip Angle (upper figures)

Mechanical Design and Fabrication

One of the goals of the project was to improve on the design, build, and testing processes that have been used in prior research vehicles like the GL-10. To achieve these goals the project utilized additive manufacturing. Proposed advantages included: low labor airframe parts, which had a high accuracy for complex geometries; mass production scalability based on additive manufacturing fabrication companies; replacement and repair parts to be made on demand. In addition to using additive manufacturing, a low cost, high speed, high moment actuator was also required to facilitate achieving the project test goals.

To begin designing the airframe, several prototypes were required to define how the parts should be connected, assembled and support expected load requirements for flight and tunnel testing. One of the first prototypes made provided specifications for how access hatches would be attached to the fuselage. One key feature was brass inserts as shown in Figure 12, which were inserted in a nylon material. This feature worked well for attaching access hatches.

Figure 12. Brass Insert Embedded Into Nylon

Another design decision in consideration was determining if the skin would be nylon or carbon fiber. Previous work indicated some potential advantages using a carbon fiber wrap, like reducing the nylon material infill needed on the part. Two prototypes shown in Figure 13 were used for comparison. Based on the surface finish and additional stiffness, it was decided to wrap the airframe in carbon fiber using a method that did not require vacuum bagging. These

prototypes also provided insight into the capabilities of the 3D printers, including part quality and print time, that the project had access to at LaRC.

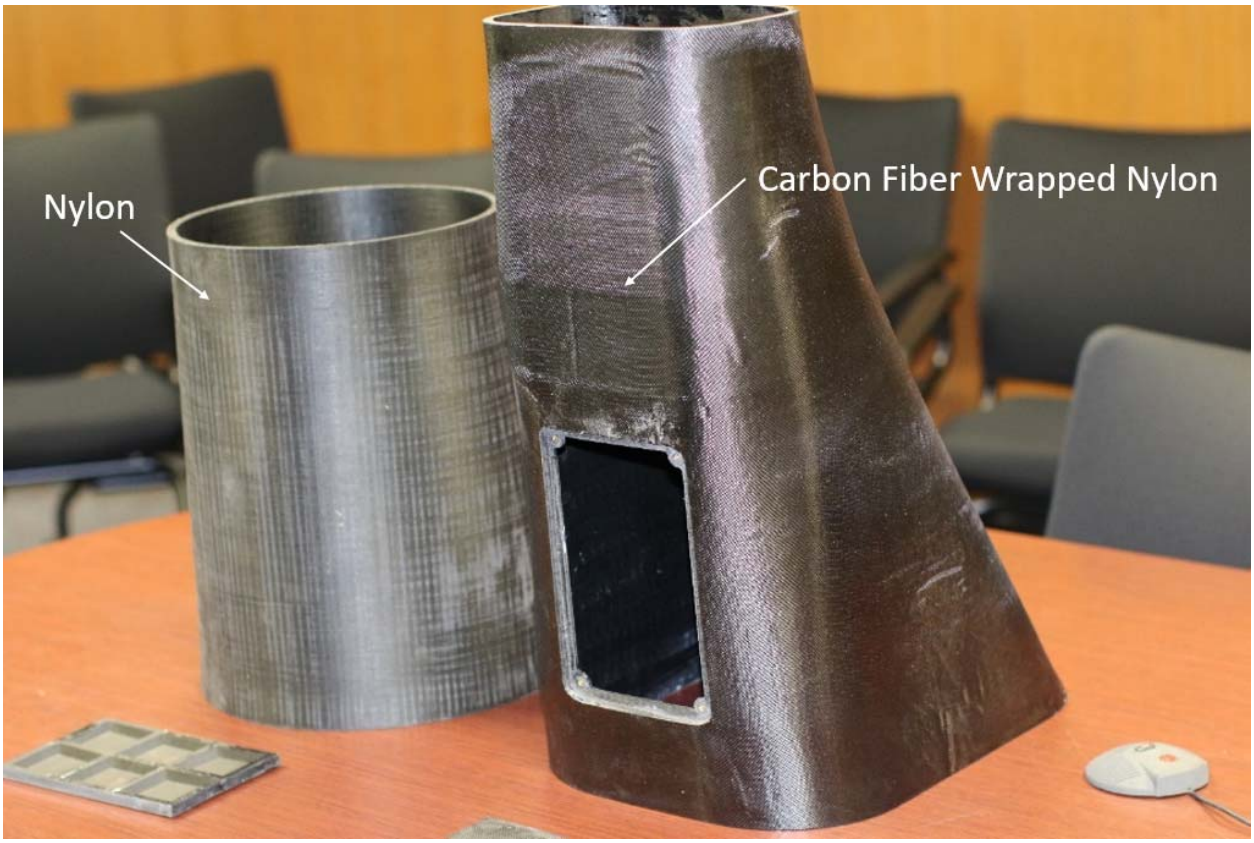

Figure 13. LA-8 Fuselage Test Parts

The airframe utilized 3 different types of printer filament: FDM Nylon 12 shown in Figure 14, Onyx shown in Figure 15, and PC (polycarbonate) shown in Figure 16. In general, the Onyx parts had the best “as printed” surface finish. The PC surface finish was better than the FDM Nylon 12, but not as good as the Onyx. The FDM Nylon 12 had the least desirable surface finish. Each of the materials provided benefits, which led to their specific use cases. The FDM Nylon 12 parts were made when the support structure was needed to be dissolved away. The Onyx parts were made when stiffness and surface finish were important, and the removal of supports did not put the part at risk to be damaged. The PC parts were made when large stiff parts with complex geometries were needed.

Figure 14. FDM Nylon 12 Fuselage Section

Figure 15. Onyx Winglet

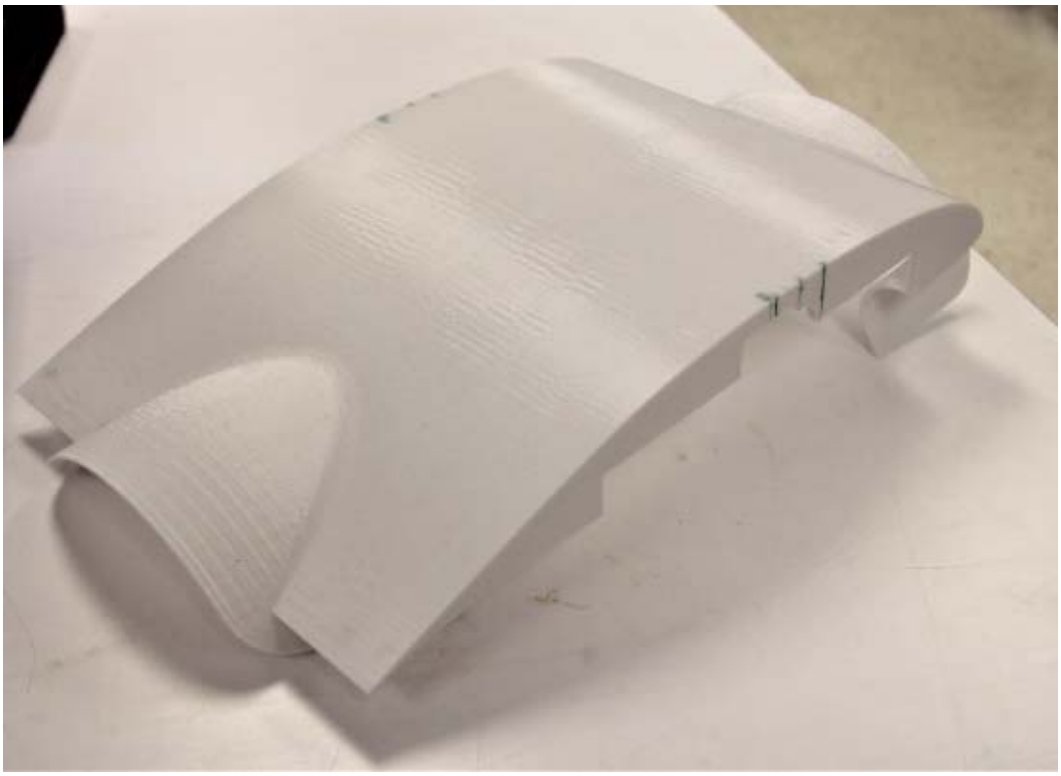

Figure 16. PC Access Hatch

When it came time to paint the parts, the polycarbonate parts were easiest to prepare for paint and required the least amount of sanding and filler after primer to achieve a very smooth finish. The nylon parts were much harder to sand when uncoated. The polycarbonate parts tended to be more stiff, but also brittle.

The fuselage was broken into six parts as shown in Figure 17. This was done for three reasons: to enable printing in the volume constraints of available printers; to allow for future configuration changes; to mitigate time and material lost if prints failed. If a design change was required, there was an opportunity to make all the needed changes to any part, reducing time for future modifications to the vehicle design. Print failures are not uncommon when printing a complex geometry for the first time while utilizing the full capabilities of the 3D printers.

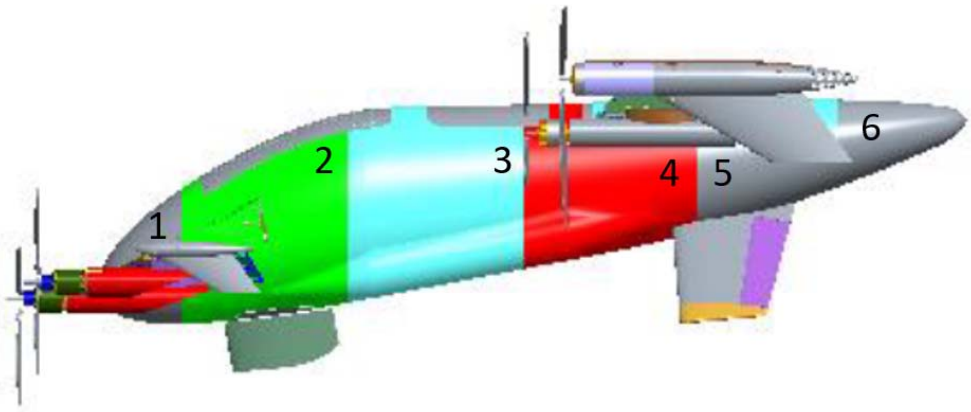

Figure 17. LA-8 Fuselage Sections

A pair of carbon fiber foam core plates 6 inches apart created the backbone of the fuselage. The 4 mid sections of the fuselage were bonded to the carbon plates to generate the primary fuselage structure. Once the 4 fuselage sections were bonded to the side foam core plates, it was determined that the structure was suitably stiff, and the need for covering the fuselage with a carbon fiber wrap for additional stiffness was not needed. NACA ducts as seen in Figure 18 were incorporated into the sides of the fuselage. The ducts allow airflow into the fuselage for cooling of power electronics.

Figure 18. LA-8 Fuselage Cooling Inlet Ducts

The nose section and tail section of the fuselage were designed to be removable for forward and aft fuselage access. The nose section also allowed the forward wing to be removed/installed. The nose section has reinforcing ribs and mounting provisions for an alpha-beta pitot probe. The tail section has a honeycomb vented section on the back for exhausting fuselage cooling inlet air. Five hatches, 2 lower and 3 upper, were incorporated into the design. The two lower hatches are for the forward landing gear bulkhead access and for the sting and balance mount hardware, when mounted in the wind tunnel for testing. The 3 upper hatches are for access to electronics systems, battery installation and removal, and aft wing installation and removal. Threaded inserts were incorporated into the carbon side panels for attachment of wind tunnel mount hardware, electronic board mounting brackets and battery support brackets. The vertical tails and landing gear were also incorporated into the fuselage. For tunnel testing and initial hover flights, a rolling landing gear system was not required and, therefore, not implemented. Initial forward landing gear consisted of an airfoil fairing mounted on the lower forward area of the fuselage. A carbon tube extends from a bulkhead bolted into the fuselage just aft of the forward wing mount area. On the rear, the vertical tails function as the landing gear. Similar to the front, the vertical tails are attached with carbon tubes secured to a bulkhead in the aft section of the lower fuselage. The aft bulkhead contains mounts for servos that drive the ruddervators via torque tubes that also act as upper hinges for the ruddervator. The lower section of the ruddervators utilize a carbon tube as a pivot pin.

The forward and aft wings were designed to be broken into six sections as shown in Figure 19. Similar to the fuselage this was done to allow printing of the wing based on printer volume constraints, and mitigate the risk for print failures. The wings were designed to have multiple carbon foam core sheet spars running down the span. A prototype seen in Figure 20 was made to determine how the printers would handle the airfoil geometry, surface finish, and also to test a proposed attachment method for the motor nacelle shown in Figure 21. The bolting method and print quality for the prototypes provided confidence to move forward with designing the wings.

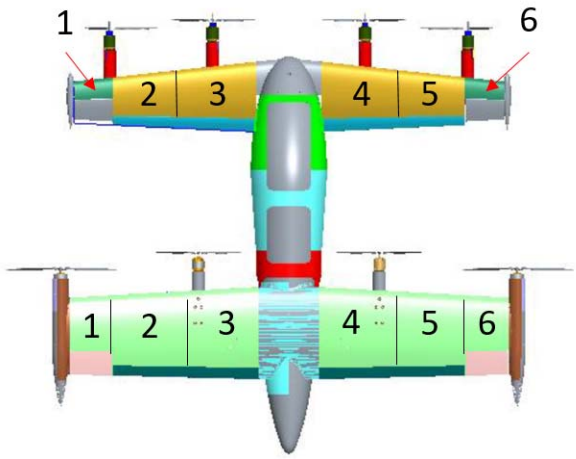

Figure 19. Forward and Aft Wing Sections

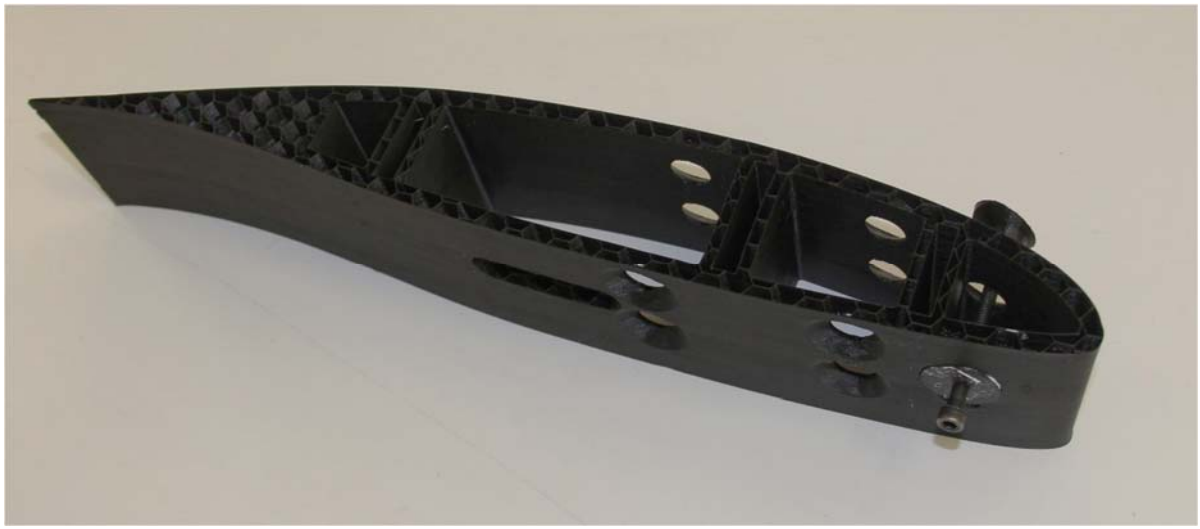

Figure 20. LA-8 Airfoil Prototype Test Part

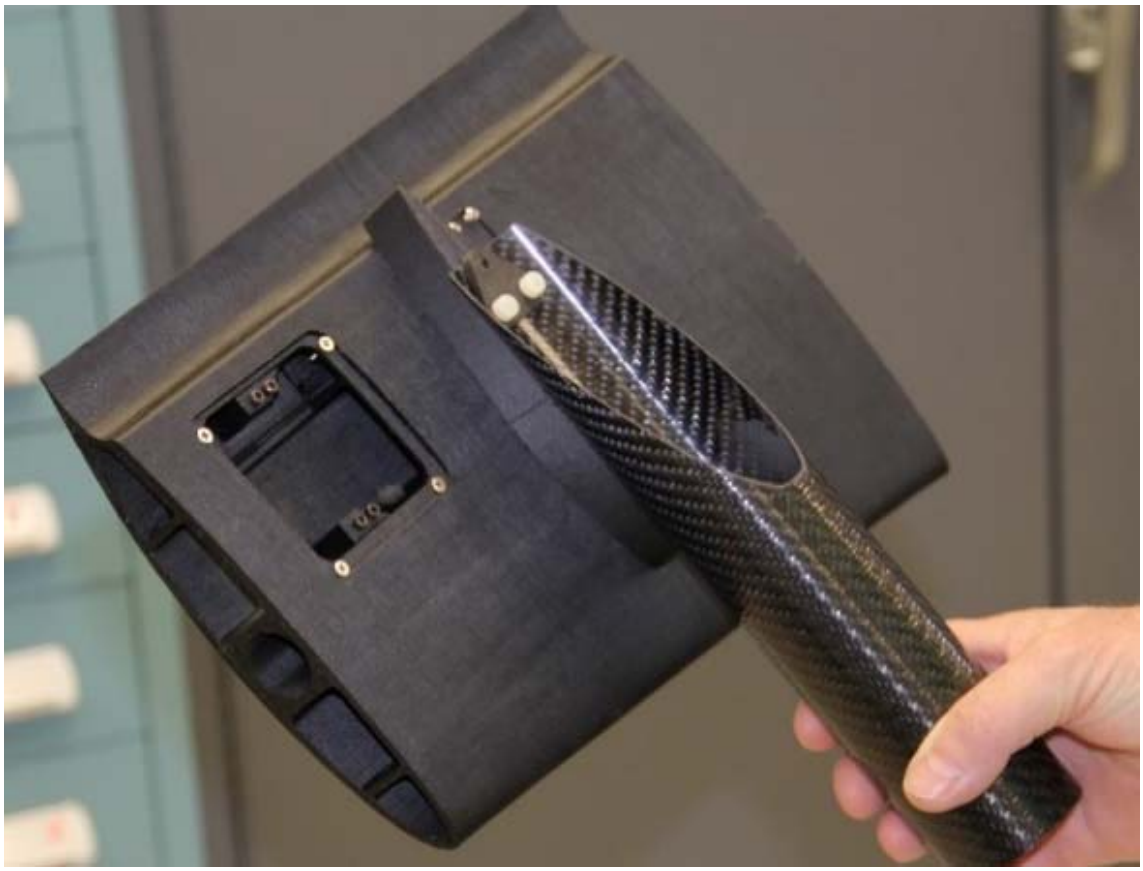

Figure 21. Nacelle Attachment Prototype

The aft main wing was fabricated into 6 sections, with additional outboard sections that doubled as a winglet and a nacelle for the outboard motors. This outboard section also contains the servo that drives the elevon directly. The servo wheel is fastened to a drive adapter that engages directly into the outboard end of the elevon, serving as the outboard hinge. For fabrication the wings were assembled as half span assemblies. The half span assembly also allowed utilization of an aluminum cylindrical spar to meet the designed wing dihedral requirements. This decision was based on simplifying the design and fabrication of the wing root and spar interface. The 3 sections were bonded together to create a half span wing with an aluminum spar bonded inside.

Due to available project resources and schedule, a decision was made to fabricate a forward wing using a hot wire machine to cut a wing section out of foam and then wrap it in carbon for strength. An assembly fixture was designed and fabricated for establishing dihedral, sweep and taper of the wings. A sample foam wing shown in Figure 22 was fabricated to be used for load testing. The wing was load tested to failure, and far exceeded strength

requirements for the airframe. Once the wing load test article was tested, a functional wing was required to be fabricated for the vehicle. The foam core wing built for the research vehicle required significantly more hands-on work compared to the load test article. The extra hand work was needed for inserting and bonding multiple ribs and hard points into the wing for motor pylons, servos, control surface hinges, and wingtips. Since the new wing design was different from the test article, an additional load test was required prior to conducting flight or tunnel testing. Although not planned, this alternate approach allows for comparison of the two different fabrication techniques: the foam core fabrication technique on the front wing and the fabrication of the aft wing which was primarily built with 3D printed components. Although a foam core forward wing was used for the first vehicle prototype, future forward wing prototypes are planned to be 3D printing.

Figure 22. Foam Core Carbon Fiber Forward Wing Load Test Article

The flaps on each wing were built in 2 sections to mitigate the longer, more slender parts that tended to warp during printing, based upon prior experience with the FDM Nylon 12 material. Span wise holes for carbon fiber tubes were designed into the flaps cross section for reinforcement. The tubes were bonded into the flap halves, then the flap halves were bonded together. The resulting flap assembly was straight and fit correctly into the wing assembly.

The wing actuation system in the GL-10 tilt-wing configuration utilized an industrial automotive linear actuator. While the GL-10 actuator provided a high force (150lb), it was heavy and slow. The GL-10 actuator was chosen because there were no readily available commercial alternatives in the size and cost range of the project. The GL-10 actuator required a large mounting bracket, and a substantial arm off of the wing pivot to drive the rotation to meet wing moment requirements. Additional compression tubes were used to tie the actuator mount bracket structure to the wing pivot structure in order to accommodate the actuator loads. The system was heavy relative to the vehicle weight and required a large volume in the fuselage. The Mechanical Fabrication and Design Team decided a custom actuation system could be designed for LA-8 that would provide the required torque, but have a faster rotation rate and smaller volume footprint. The design goal was to use an off the shelf RC servo that would be powered and controlled similarly to the other servos on the LA-8 model. The primary criteria considered during the LA-8 wing actuator design included the maximum torque, the wing range of rotation, and the speed required to translate from one end of the range to the other.

For the LA-8 wing drive mechanism seen in Figure 23, two side plates were designed that would support the primary drive shaft, secondary drive shaft, and tie to the driven carry though shaft. These side plates were machined out of aluminum. The primary and secondary shafts rotate on steel needle bearings. The final drive/wing carry through is supported on nylon sleeve bearings. The primary shaft is attached to the servo utilizing an aluminum shaft adapter that is fastened to the servo "wheel" with socket head cap screws. The output bearing in the servo doubles as the bearing for the shaft on one end. The other end of the shaft is supported by a steel needle bearing in the side plate. The primary gear is on the end of the shaft closest to the side plate in order to transfer most of the gear load into the roller bearing and not into the servo. The secondary shaft is supported by needle bearings on each end. The gears are secured to the shaft with set screws. The side plates are connected at the carry through end with a bearing cap that attaches to both side plates and houses the nylon sleeve bearings. The other end of the side plates are connected with a tie plate that transmits the rotational loads into the fuselage structure. The tie plate was fabricated from 1/8 inch carbon fiber plate.

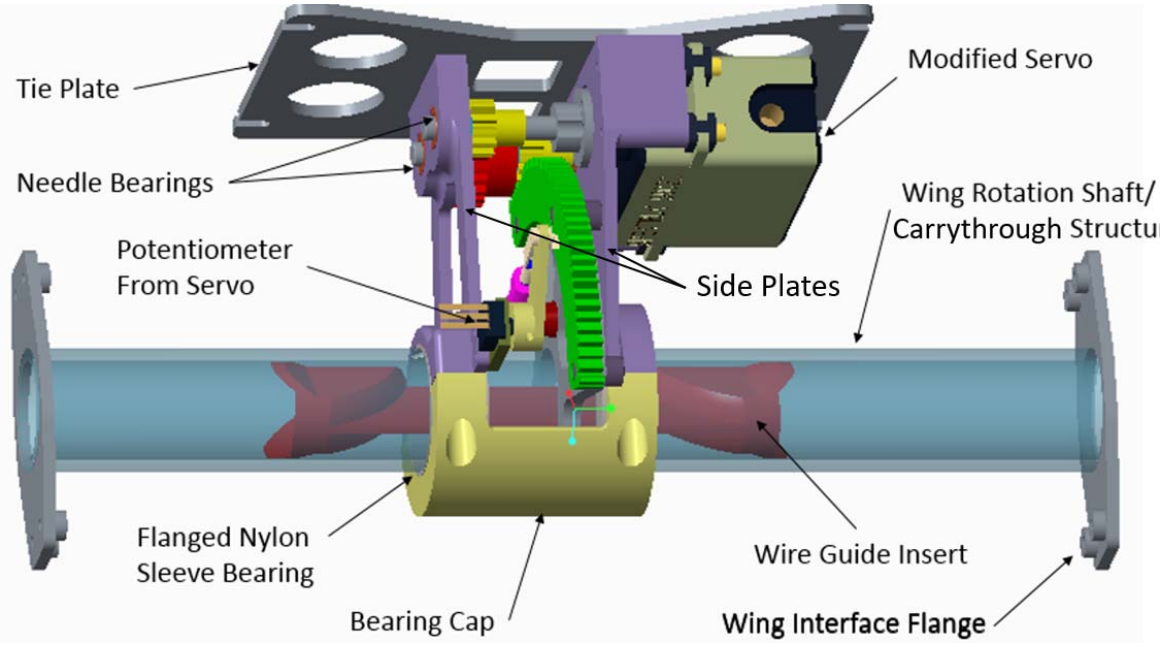

Figure 23. LA-8 Wing Actuator Design

The GL-10 actuator had the same torque (5000 oz-in), range (90 degrees) and speed (10 sec) requirements as the LA-8 actuator. The weight of the GL-10 actuator and associated hardware totaled 4.0 lb, the LA-8 wing drive assembly and associated hardware shown in Figure 24 is 1.9 lb which includes the wing carry through structure. If you remove the weight of the carry through structure, which is part of the wing on the GL10 airframe, the weight of the LA-8 wing drive is 1.4 lb. This results in a weight savings of 2.6 lb or 65% compared to the GL-10 actuator. The LA-8 airframe has a forward and aft wing and requires 2 wing drive assemblies. Total weight savings over the GL-10 actuator system is 5.2 lbs. With a target airframe takeoff weight of 55 lb, this results in a reduction of over 11% of the airframe weight, allowing for more payload or batteries. The compact size of the drive relative to a linear actuator also frees up valuable space in the fuselage for other electronic components.

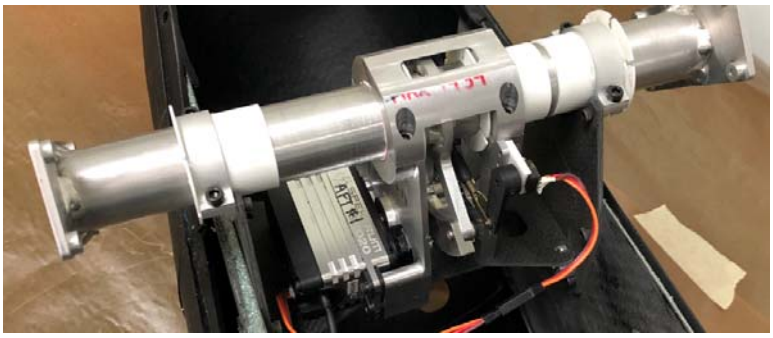

Figure 24. LA-8 Wing Actuator

Electronics Design and Fabrication

An electronics system was designed by the Electronics and Data System Team utilizing low cost commercially available products, which would support flight testing of the research vehicle concept. The system is comprised of four sub-systems: Control, Data, Power, and Auxiliary.

The LA-8 control system was developed based on three RC Flight Controllers (FC) in parallel connected to four RC Multiplexer (MX) boards. Based on experience utilizing OpenAeroVTOL from GL-10 flight testing, it was determined the KK board flight controller had the capability to support transition modes of operation, but lacked the number of outputs needed to provide independent control of all desired control surfaces, motors, and wing actuators. An idea to put multiple controllers in parallel to enable 20 outputs was proposed to meet the need for a low-cost baseline controller with a minimum of 20 independent control outputs. This idea had risk associated with the independent controllers interfering with each other during the various flight modes, therefore a prototype test vehicle shown in Figure 25 called Langley Aerodrome 7 (LA-7) was designed and built to provide some insight into the feasibility of utilizing three controllers in parallel running OpenAeroVTOL firmware. LA-7 vehicle specifications can be seen in Table 1.

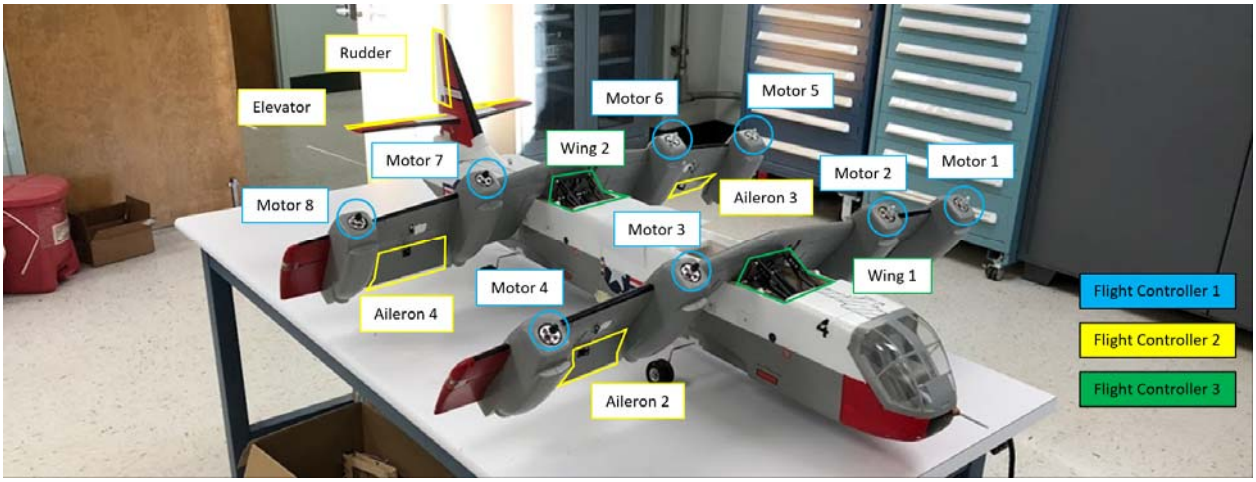

Figure 25. LA-7 Control Architecture

Table 1. LA-7 Specifications

Langley Aerodrome 7 (LA-7)	
UAS Type	VTOL Tilt-wing, 8 Brushless Motors
Wingspan	47 in
Wing Area	658 in^2
Mean Chord	7 in
CG Station	40% between forward and aft wing
Empty Weight	10 lb
Max Take-Off Weight	13 lb
Battery	2x5212mAh 6-cell Li-Poly
Operating Frequency	2.4 GHz ISM
Radio Range	1 NM
Command and Control	Remote Control Transmitter, Spektrum
Telemetry	900MHz, 100mW
Crew Requirements	Pilot, Ground Station Monitor, Spotter

Several flight tests were conducted utilizing LA-7 to verify the control architecture. The first flight of LA-7 was a hover inside an outdoor net located in the NASA LaRC CERTAIN range shown in Figure 26. The flight test was to verify control in multi-rotor mode was adequate. Any undesired oscillations were corrected by adjusting the FC PID parameters. Once hover testing was complete with no major issues, the team moved onto transition testing in the NAS at CERTAIN, which can be seen in Figure 27. Several flights tests were conducted transitioning from multi-rotor mode to 75% transition. No issues were observed during the first 75% of the transition. No undesired pitch or roll oscillations were observed up to 75% transition. During flight testing between 75% and 100% transition, LA-7 lost pitch control and was damaged. It was assumed that the C.G. location was the reason for the pitch axis loss of control, but there was no observed oscillations that would indicate the flight controllers had control conflicts during transition.

Figure 26. LA-7 CERTAIN Net Hover Flight Testing

Figure 27. LA-7 CERTAIN Transition Flight Testing

Two outcomes of this test were needed before moving forward with the LA-8 electronics design. The first was determining that putting all motors on a single controller, and all the control surfaces on the remaining controllers enabled adequate control authority and responses in multi-rotor mode, transition mode and airplane mode. The second was determining that the latency added into the control system from the addition of multiplexer switches did not cause control problems. The multiplexers were desired because they would allow the ability for flight testing and wind tunnel testing utilizing an independent research controller board if desired or needed. Based on ground tests and flight tests, the RapidPACT team determined it was feasible for the three FC's and MX switches to support flight testing of the LA-8 vehicle.

In the control system diagram shown in Figure 28, a single RC Receiver (RX) would allow an external pilot utilizing a remote control transmitter to send command and control signals to the FC for baseline operational manual capabilities. The three FC's would all receive the same commands, but are programmed for their different actuator/effector outputs. FC outputs listed in Table 2 were assigned for each of the FC's. The motors were controlled by electronic speed controllers (ESC1-ESC8), which interfaced via an ESC Interface (EI1-EI8). These interfaces were small single board computers that were sold by the manufacturer of the ESC. The Servos (S) required three different voltages: 12 volts, 8 volts and 5 volts. These all required a separate regulated voltage supply, which is covered in the power system description. The Digital Isolators (DI) are discussed in the auxiliary system description below.

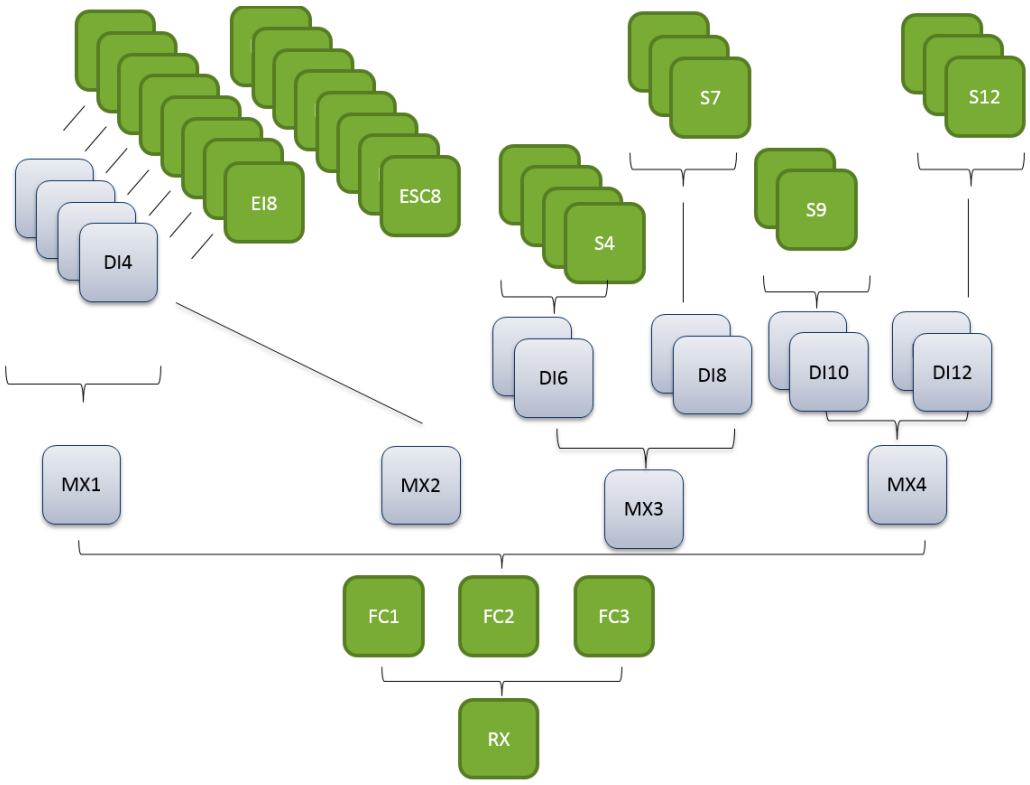

Figure 28. Control System Architecture

Table 2. LA-8 Flight Controller Output Assignments

	FC1	FC2	FC3
Output 1	Motor 1	Elevon 1	Flap 1
Output 2	Motor 2	Elevon 2	Flap 2
Output 3	Motor 3	Elevon 3	Flap 3
Output 4	Motor 4	Elevon 4	Flap 4
Output 5	Motor 5	Ruddervator 1	
Output 6	Motor 6	Ruddervator 2	
Output 7	Motor 7	Wing 1	
Output 8	Motor 8	Wing 2	

The data system shown in Figure 29 was designed to collect performance data and aircraft health prognostics. The main controller of the data system was Single Board Computer (SBC) 1. This board had the function to coordinate and request data from the other SBC's (SBC2-SBC4). The communications between the SBC's was RS-485. RS-485 was chosen because of its robustness and reliability for data communications in the system. The Analog Inputs (AI) and Differential Analog Inputs (DAI) consisted of 8 analog to digital boards (A-F) which transmitted their analog input data over SPI to SBC2. Airspeed (AS) 1 provided air data to SBC3 over I^2C. ESC Interface (EI) provided motor data to SBC3 over I^2C. PPM Encoders (PE) transmitted Pulse Width Modulation signals to SBC4. The Inertial Navigation System (INS) provided vehicle state information to SBC1 over RS-232. RS-232 was used because the INS natively supported that communication bus. Radio (R) 1 provided a telemetry link to get the flight data off the vehicle to a ground station computer for real time analysis, health monitoring and recording.

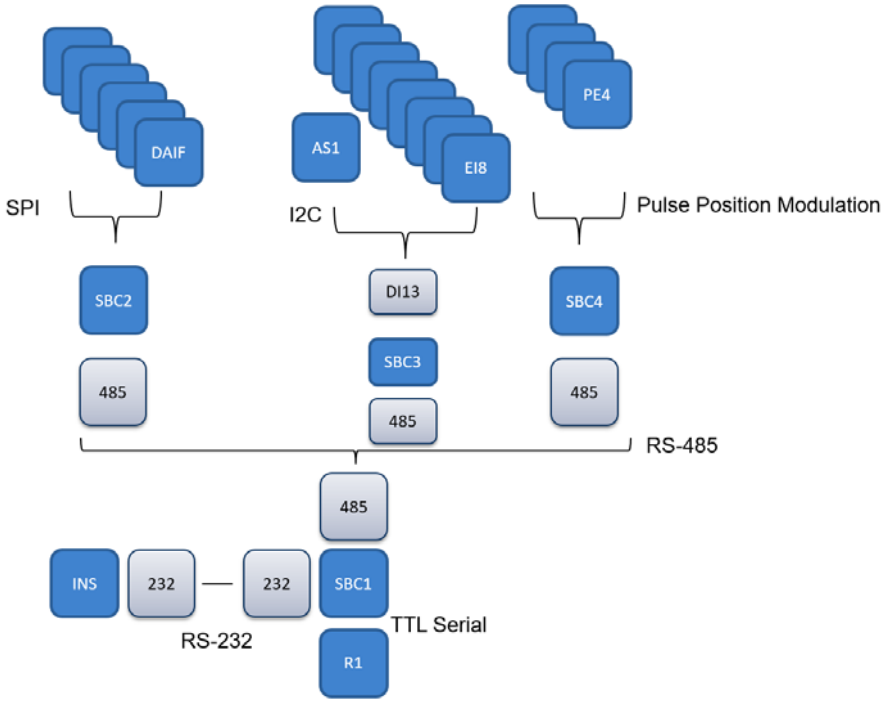

Figure 29. Data System Architecture

A low cost air data probe prototype as seen in Figure 30 was designed to support initial high risk flight testing. The air data probe design focused on ease of manufacturing and measurement of a large angle of attack for transition airflow. This desire came from previous GL-10 flight test data which did not have enough range from the air data system to include the majority of the transition. Vanes and magnetic encoders were used to provide a large angle of measurement. This air data probe was designed to be used during initial high risk flight testing.

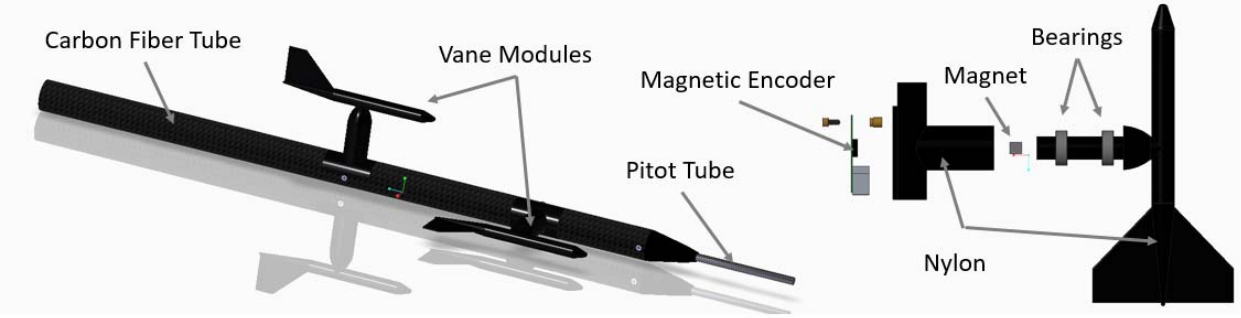

Figure 30. Custom Low Cost Air Data Probe

A prototype, shown in Figure 31 was built and tested on a laboratory workbench. The initial results using a multimeter to check sensor analog output looked promising. Angle measurements were repeatable, with an accuracy of 1-2 degrees. The range of the prototype air data probe was approximately 90 degrees.

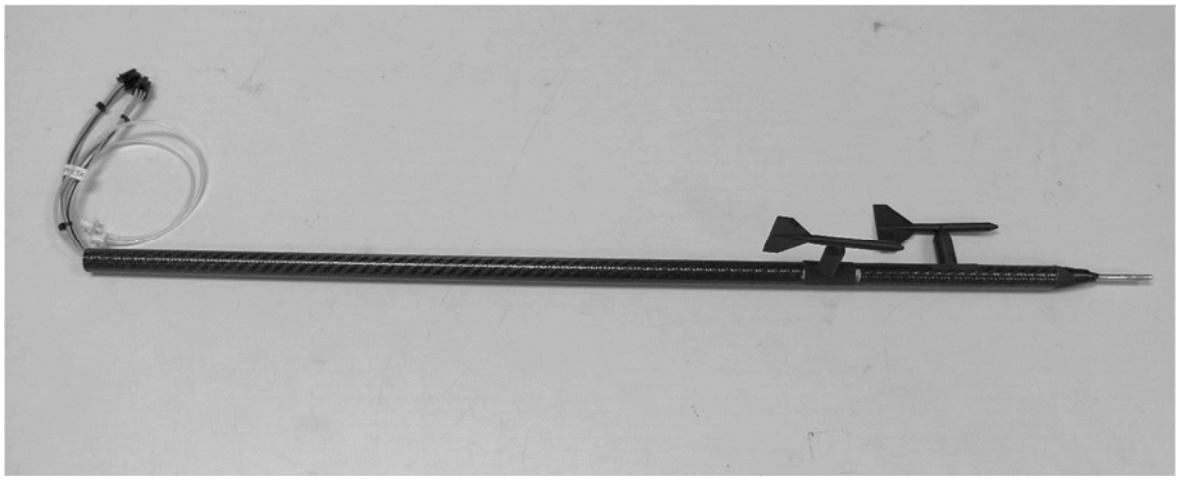

Figure 31. Low-Cost/High Angle Alpha/Beta Probe

The designed analog data architecture shown in Figure 32 enabled modular analog inputs. Based on this, a nomenclature was established to allow recording of inputs that could be mapped to what the data was outside of the system. Therefore, Analog (A) input number (1-8) and the associated board (A-F) was used to identify each unique input within project documentation. Voltage Divider (VD) 1 was used to record the vehicle main power voltage from the analog inputs, which only supported up to 15V inputs.

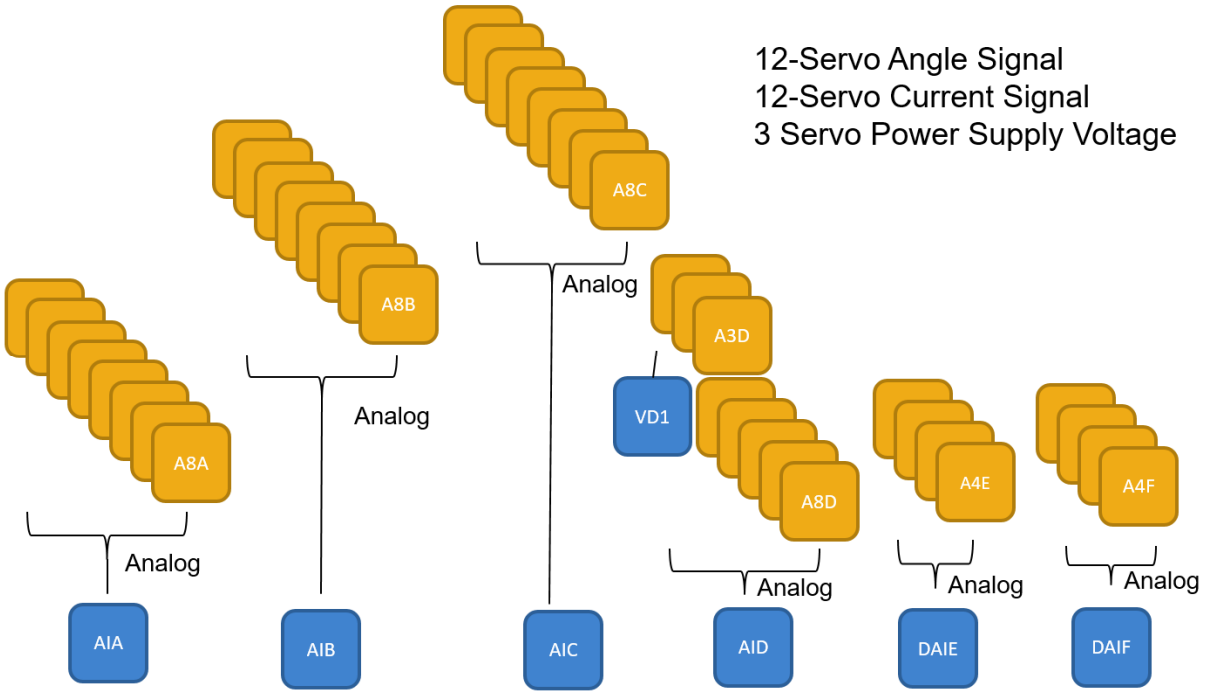

Figure 32. Analog Input Nomenclature Assignments

The power system architecture, shown in Figure 33 was designed to support a battery failure, and to account for thermal considerations for heat generated by the ESC's. The system components include: Batteries (B1-B2), Schottky Diodes (ZD1-ZD2), Power Distribution Bus (PDB1), Voltage Regulators (VR1-VR5) and cooling Fans (F1-F4). To provide the required thrust per motor requirements, 33V (8S) LiPo batteries were selected in conjunction with the motors and propellers. The diodes selected prevent a failed battery from acting as a load in the system. Based on the heat generated by the diodes and ESC's, cooling fans were provided to address thermal concerns. The power distribution bus is comprised of two copper bars, which were water-jet cut, in order to allow all loads to be connected directly to the copper bus bar. This decision was based on experience with the GL-10 power distribution bus, which had high temperatures on terminal connections that provided power to multiple ESC's. The copper bar also provides a heat sink to address thermal concerns. The voltage regulators were low cost commercial products and were chosen because of their ability to be programmable.

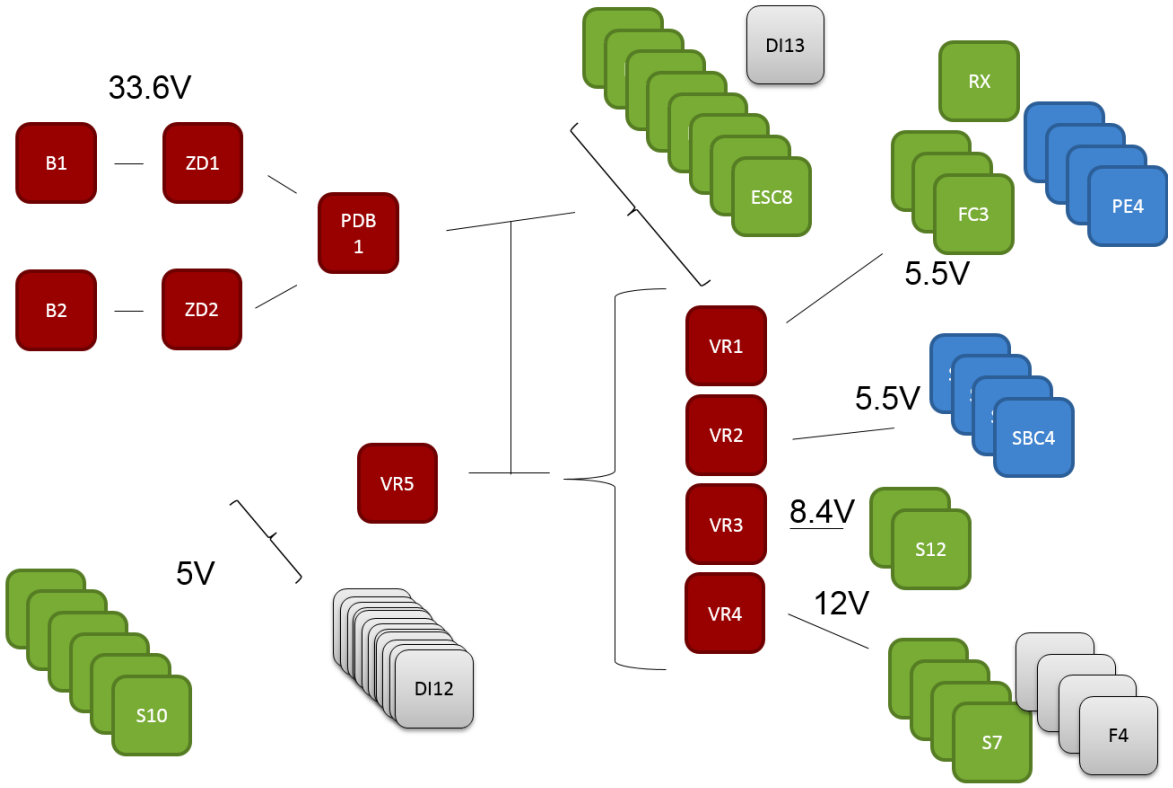

Figure 33. Power System Architecture

The auxiliary systems were designed for two functions: To allow the motors and servos to accept commands from two independent control systems (Flight vs. Tunnel Testing); to allow electrical isolation between the flight control system and the motors, actuators and data recording components. Some confidence for the implementation of the FC1-FC3 and MX1-MX4 was established during flight testing conducted utilizing LA-7. As previously stated, the three FC's were required for enabling 24 controller outputs, and the MUX's were required for enabling a secondary controller system to interface with the vehicle actuators/effectors. When using the multiplexers, the RC transmitter would have the ability to determine if the secondary controller should have command of the motors and servos. Digital Isolators were used (DI1-DI12) to keep the motors and servos electrically isolated not only from the flight controllers, but from one another.

After the electronic system was designed the next step was to model all the components and place them inside the fuselage to determine physical location and integration. This was completed in a CAD program by importing two 2D vehicle layout images (Top View, Side View) shown in Figure 34. In this figure you can see the green control system components and

the red power system components. Additionally, several auxiliary components can be seen in white, including fans and isolators. The data system was defined as blue.

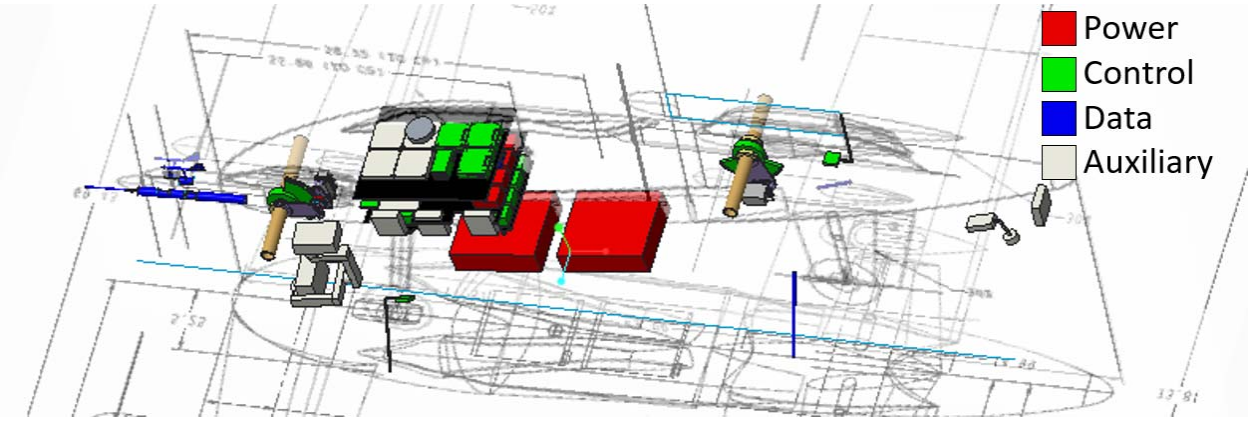

Figure 34. Electronic System CAD Model

The electronics system is physically assembled in two sub-assemblies. These assemblies include the upper tray shown in Figure 35 and the lower tray shown in Figure 36. The flight controllers were located on the aft section of the upper tray in order to get them as close to the designed vehicle center of gravity as possible. The remote control multiplexers were located forward of the controllers and as close as possible to minimize control signal harness wiring. There are two additional trays above the upper tray, which were to be used for data system components.

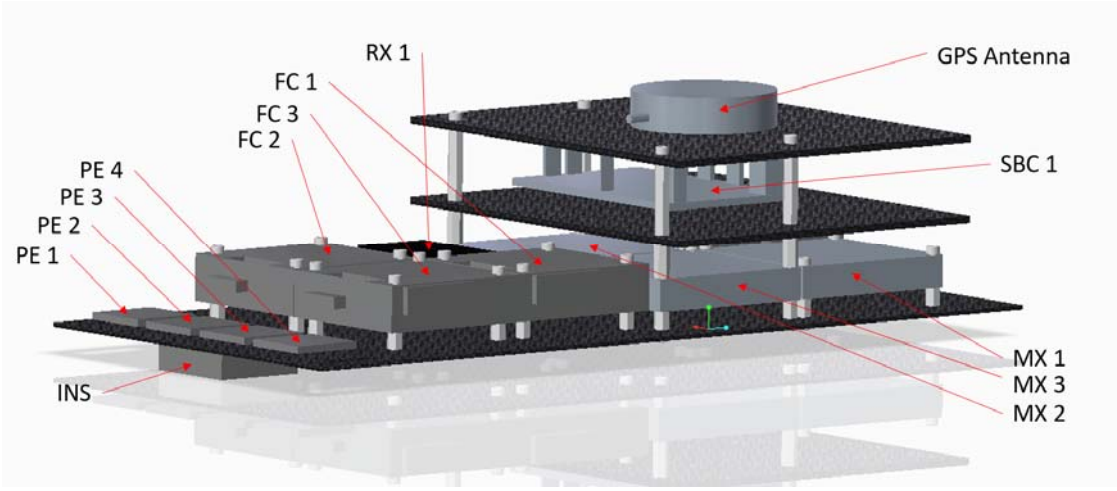

Figure 35. LA-8 Electronics Upper Tray Assembly

The lower tray is designed to keep the power components as close as possible. The electronic speed controllers are located on either side of the power distribution bus. The positive bus bar on the power distribution bus also supports room for the diodes and current sensors. The design also includes fans which will be mounted along the side to provide forced air flow over heat sources to include electronic speed controllers and diodes. The voltage regulators are positioned toward the aft end of the bottom tray within close proximity to the power distribution bus. Three custom printed circuit boards were built into this assembly to provide mounting and electrical connections for digitally isolating the motors and servos from the flight control, and data systems.

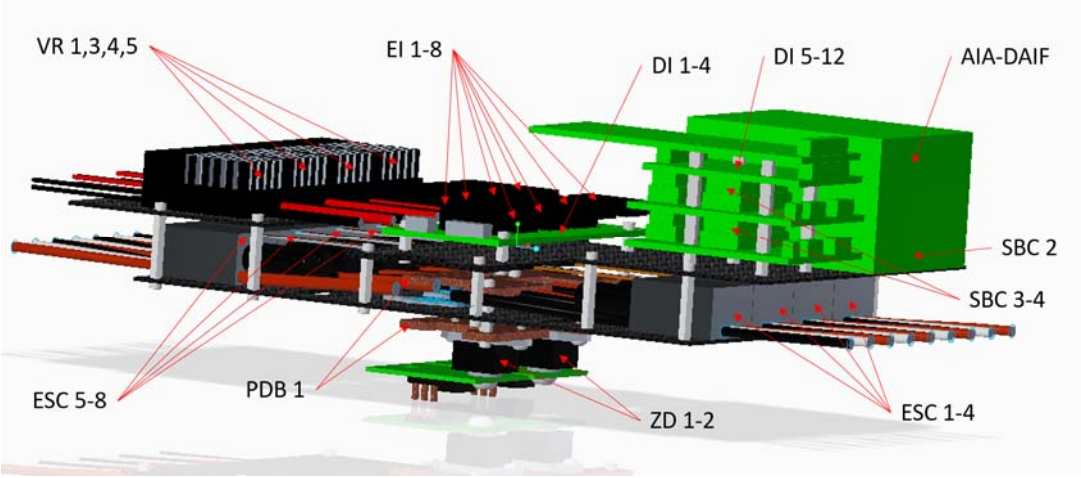

Figure 36. LA-8 Electronics Lower Tray Assembly

The width of both the top and bottom assemblies were set to 6 inches to allow them to drop into the fuselage as shown in Figure 37 through the forward top access hatch. These assemblies are secured in the fuselage using screws and “L” shaped carbon fiber brackets. Consideration was included to provide access to the screws that secured the trays to the fuselage via the access hatch.

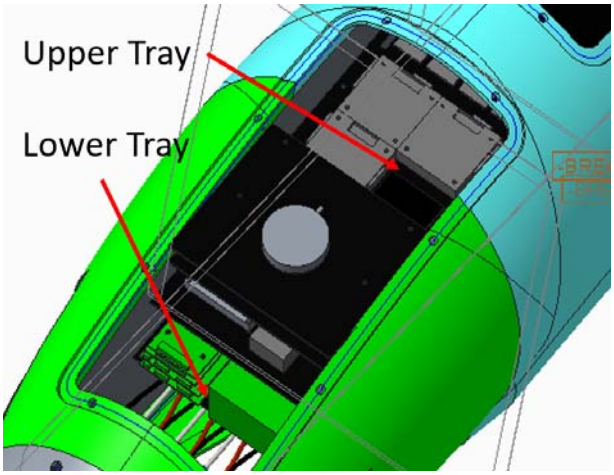

Figure 37. Upper and Lower Trays Located in the Fuselage

After the assemblies were placed in the model, an electronic system review was conducted to collect input from personnel outside of the Electronics and Data System Team on the proposed electronic system design. This review was held in the NASA Langley Engineering Design Studio and facilitated gathering feedback from across the center. No major design changes were recommended for the electronic system during the review, therefore fabrication of the electronic system began in March of 2018. All control and power system components were ordered and fabricated over several weeks. Once all hardware was on hand, and physically mounted to the trays, harnesses were fabricated. Custom harnesses were made based on electrical schematics generated through electrical design software. These harnesses were cut to length based on the mounted components and best routing determined as the electrical system was built. After the harnesses were completed, settings on the flight controller board and electronic speed controllers were configured. Figure 38 shows the first harnesses and electronics built for lab testing of the data sytem. The electronic speed controller interfaces were setup to communicate with the data system (SBC 3) utilizing I^2C. Special I^2C digital isolators were used to enable electrical isolation from the data system to the electronic speed controllers.

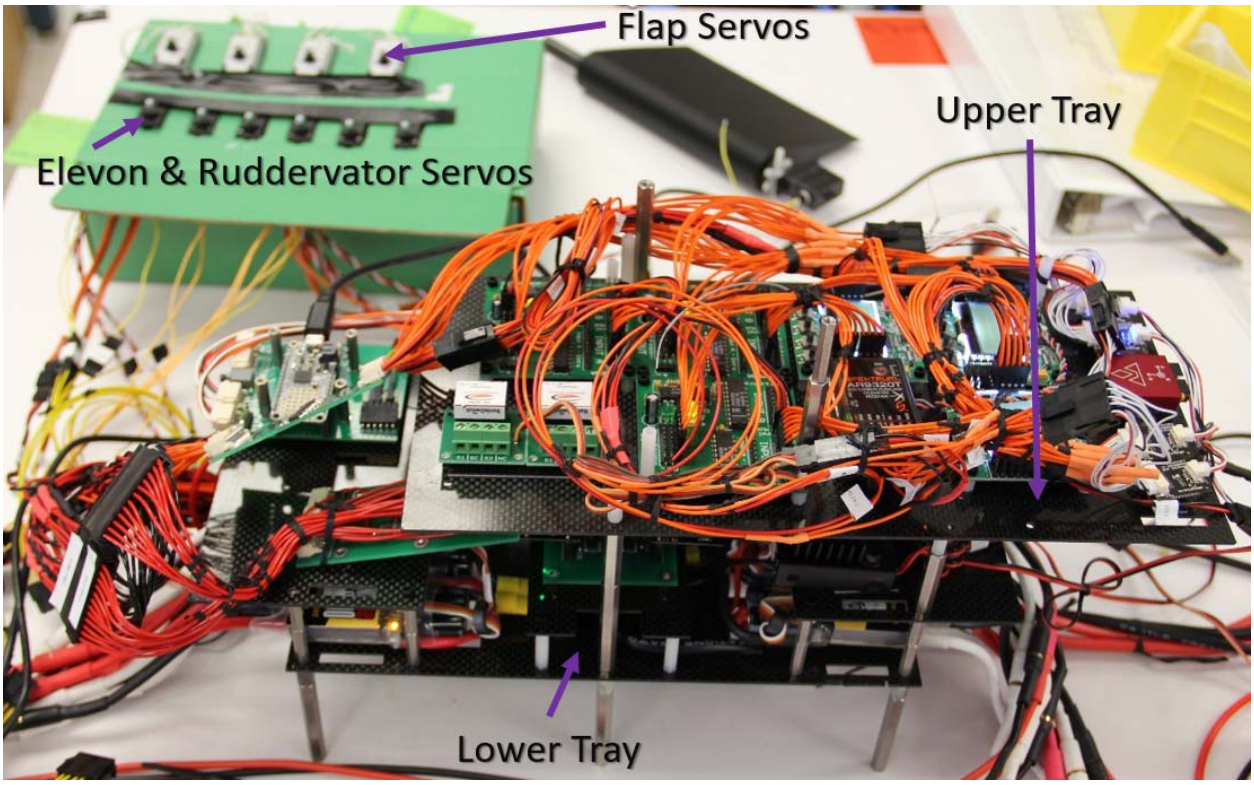

Figure 38. LA-8 Upper and Lower Tray w/Harnesses

Because there was a parallel effort to design and build the airframe and electronics, a fit check utilizing the electronics hardware was conducted prior to the final assembly of the fuselage structure as shown in Figure 39. Not only did this verify that the avionics system would fit into the fuselage, it also provided insight into the harness routing and associated access requirements based on connector locations.

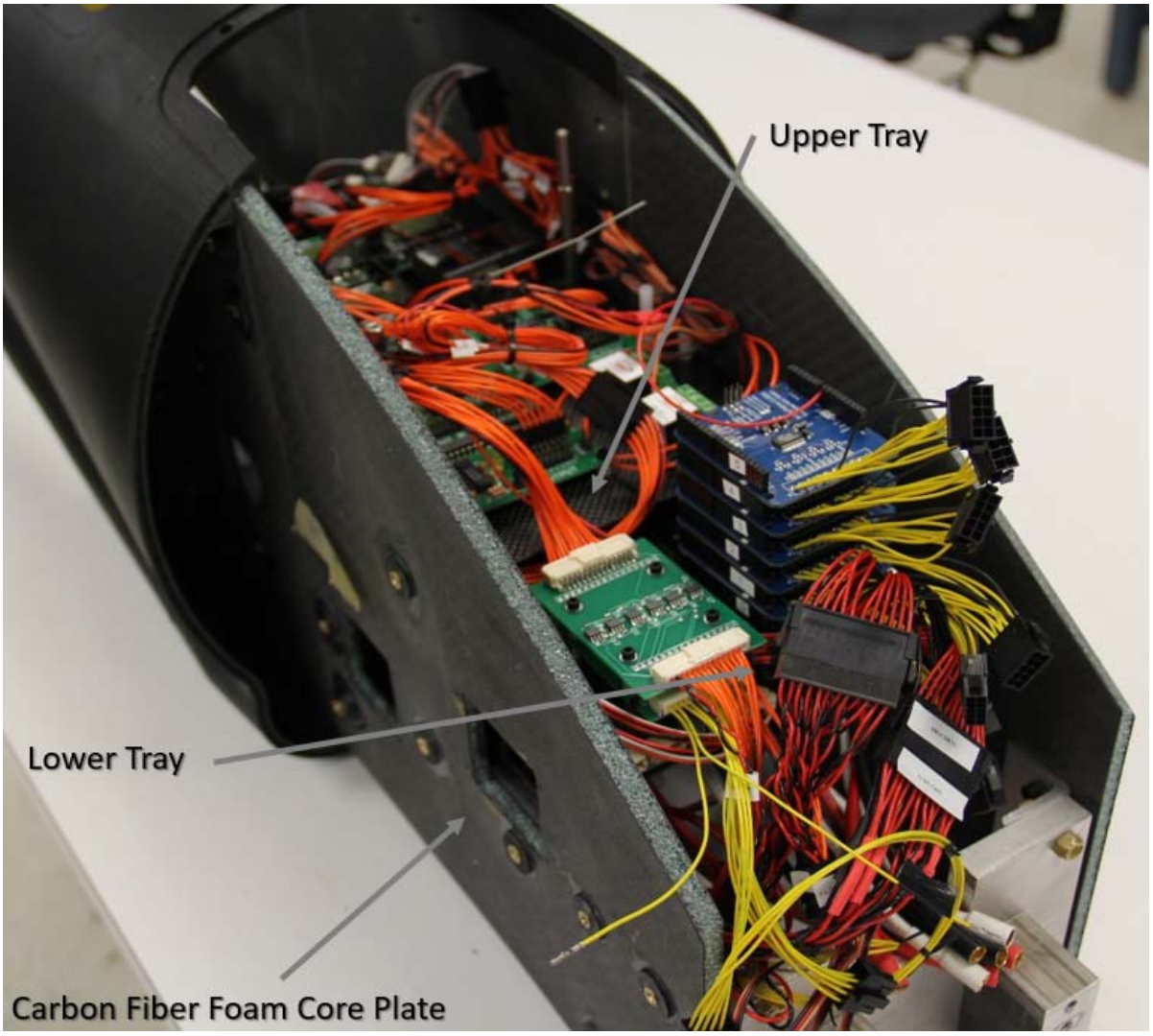

Figure 39. Electronics and Mechanical Integration Fit Test

Ground Testing

A thrust/power test for the vehicle propellers and motors was conducted in static conditions. The data provided inputs into the design of the electronics power system and also verified the available thrust met the thrust requirements for the vehicle design in static hover conditions. The aft wing-tip propeller was designed to have a 22 inch diameter. Another consideration was based on reducing tip speeds, so a three bladed propeller was chosen. A 21.5 inch diameter with a 7.5 inch pitch three bladed multi-rotor propeller was procured to support wind tunnel testing. The propeller was designed for multi-rotors, but was considered acceptable for near term research needs since the primary goals for tunnel testing were focused on blowing the wings at zero to low airspeeds with high wing incidence angles. The propellers produced approximately 14 lb of thrust in static conditions based on 33.5 volts at 38 amps shown in Figure 40.

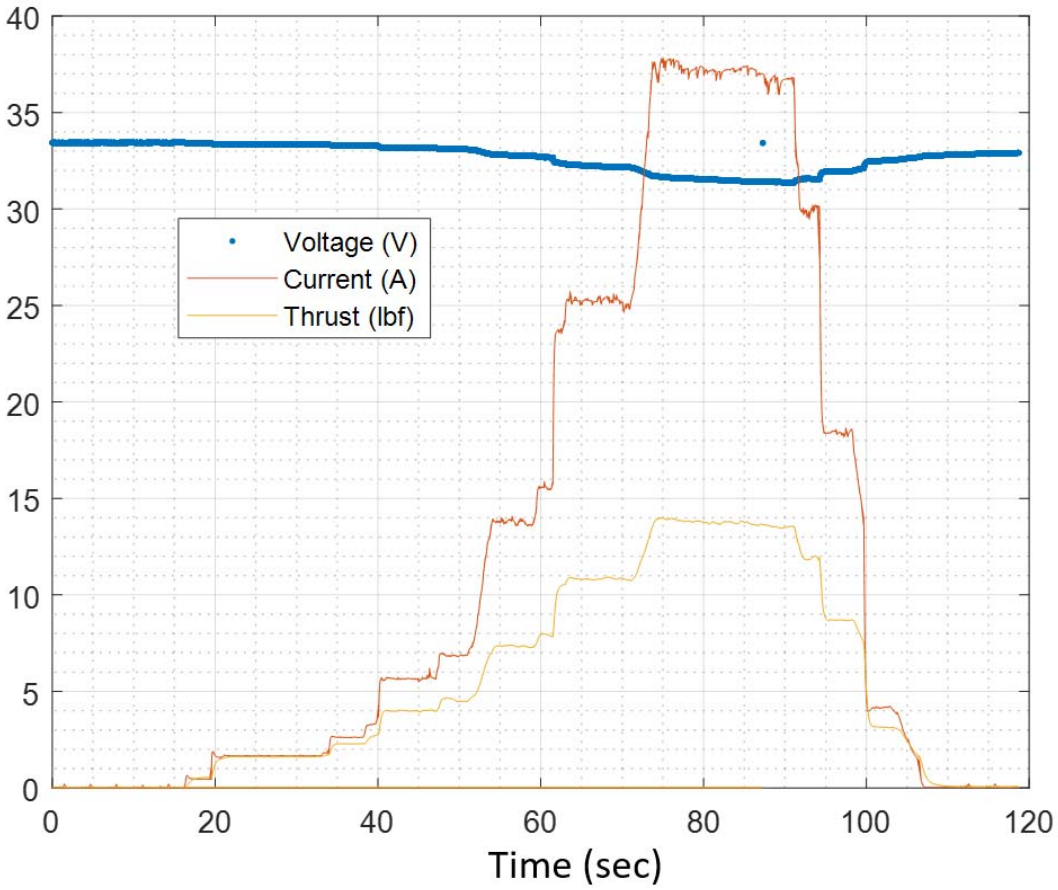

Figure 40. 21.5x7.5 inch 3 Bladed Propeller Static Thrust Data

The other propellers for the vehicle were specified to be a 16 inch diameter with an 8 inch pitch, which were previously used with the GL-10. This propeller had a pitch that was a compromise for both hover and fast forward flight conditions. Additionally, there was dynamic test data up to 80 ft/s airspeeds available for the GL-10 propellers. The 80 ft/s airspeed dynamic data showed the propellers produced 3.5 lb of thrust at 21.5 V and 33.5 A. The static data shown in Figure 41 showed the propellers produced 17 lb at 33.5 V and 105 A per motor. The static data for both propellers also provided an estimated ESC PWM input value as a function of thrust. This would be used for future wind tunnel testing and flight testing.

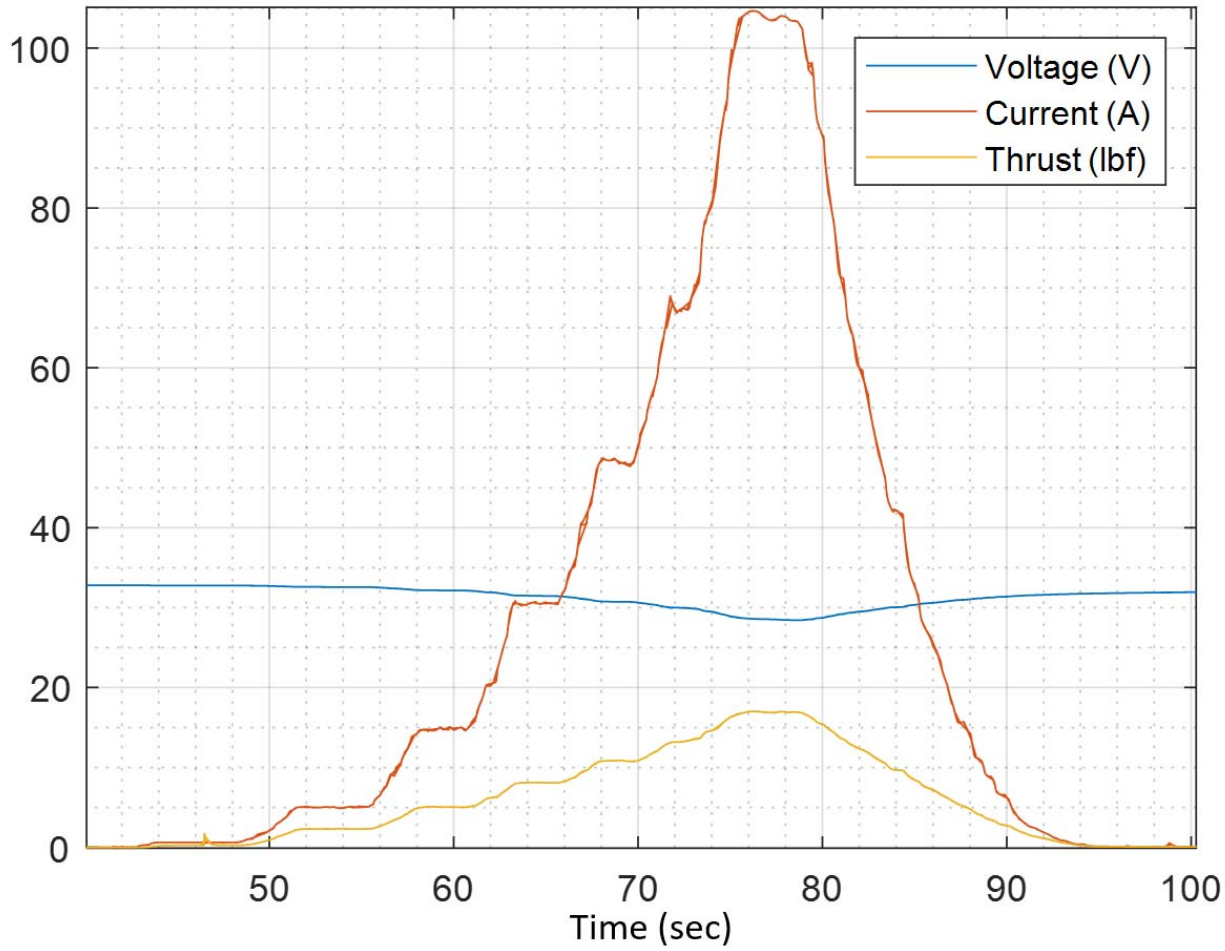

Figure 41. 16x8 inch 3 Bladed Propeller Static Thrust Data

A ground test was completed for the wing actuator which can be seen in Figure 42. Two servos were utilized in the test, in order to provide some options in the event one or both didn't have the required performance. Initial testing utilized a higher speed, lower torque servo. Gear sets were setup with a 20:1 ratio. Assuming a 20% loss of power through the gear set, the predicted torque was calculated to be 7168 oz-in. A bench test assembly was built using

aluminum side plates separated with standoffs. Shafts were fit to the side plates and rode directly in the aluminum with no bearings. It was quickly observed that the system could not generate the torque estimated. The servo could hold steady with a load of 5600 oz-in applied to the output shaft, but could only drive the system at around 3200 oz-in. This indicated the servo could be used for one third of its advertised torque rating in the wing actuator design.

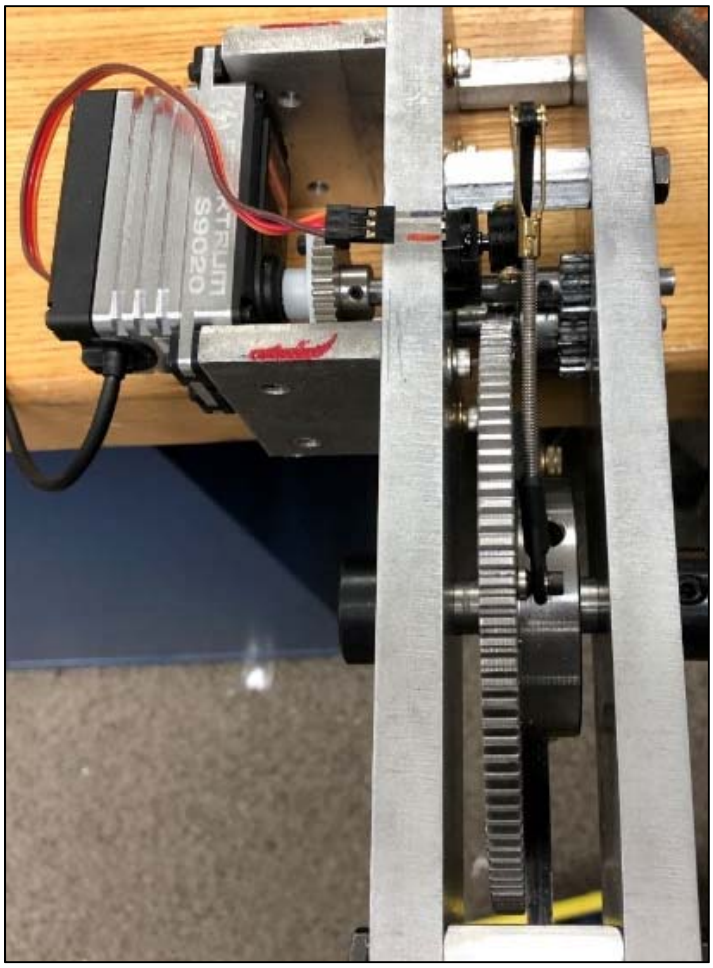

Figure 42. Wing Actuator Moment Test Setup

The higher torque servo was originally planned to be tested with a 10:1 ratio gear set, but after realizing the measured torque performance was lower than the manufacturer specified torque, the decision was made to test it with the same 20:1 gear set used with the previous servo. The servo was tested above the required 5600 oz-in requirement and performed adequately. The speed was less than anticipated, but still met the requirements. The highest load applied was 5789 oz-in, as seen in Figure 43. The system could hold steady with the power supply set at 8 volts, yielding a current draw of 2.7 amps. To drive the system at the same load, the current required was 3.4 amps. The end result of testing provided a performance capability for the wing actuator that met or exceeded the performance requirements to be utilized in LA-8.

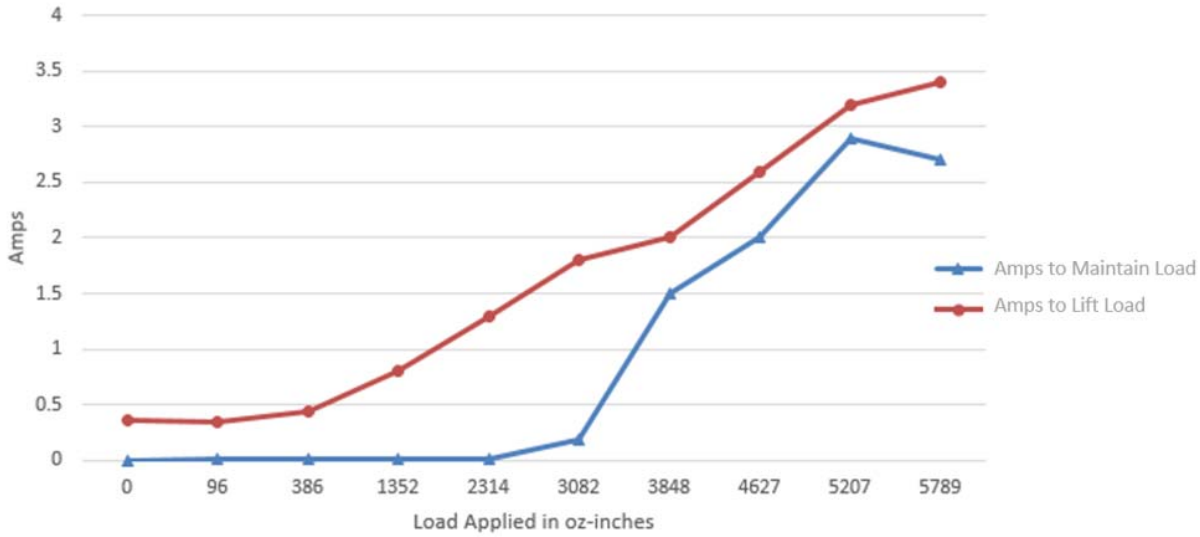

Figure 43. Drive Assembly Driven @ 8.0V

Data system communications bus testing was also conducted to verify the bandwidth could support flight data requirement rates. The results of testing provided an indication that the bandwidth was not sufficient for getting all the required data at the desired rate. Based on this, the decision to switch from RS-485 to CAN was made. The CAN data packet to be used is currently in development, and is planned to be completed before flight testing. A custom designed electrical isolation board was also tested. The isolation board provided electrical isolation between the ESC's and the SBC3. This board was needed based on experience with ground loop problems during GL-10 ground testing on the DELIVER project. The results of the testing indicated the board was functioning and made the I^2C bus reliable during motor operation.

Once the avionics system was setup, an additional test setup shown in Figure 44 was used to verify proper operation of the system before installing into the fuselage. This test rig comprised of 8 motors connected to their associated electronic speed controllers with approximate wire lengths that they would see in the vehicle. Motors on either side of the aluminum bar were connected to the electrical system to test for proper operations. After testing was completed and motors functioned as intended, the electronic system was ready to be integrated into the fuselage.

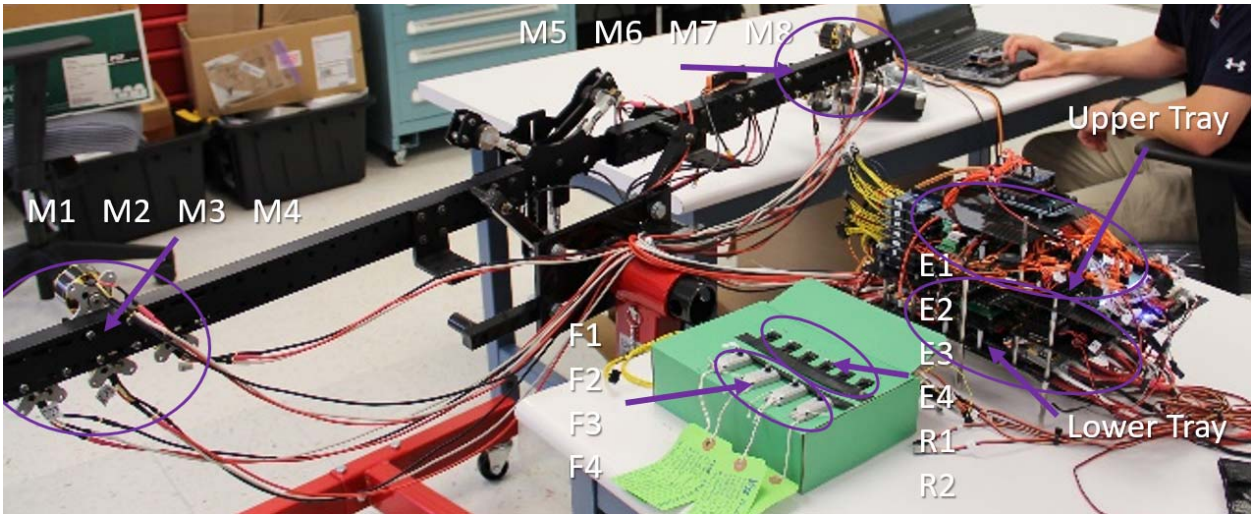

Figure 44. Control, Power and Auxiliary Systems Ground Test Setup

After the electronics were integrated into the fuselage, a control surface test was conducted as shown in Figure 45. The purpose of this test was to verify that all of the control surfaces functioned as expected. After the test a spreadsheet of servo PWM values as a function of deflection angles was completed. This spreadsheet would establish the maximum and minimum values to be used for future testing of the vehicle.

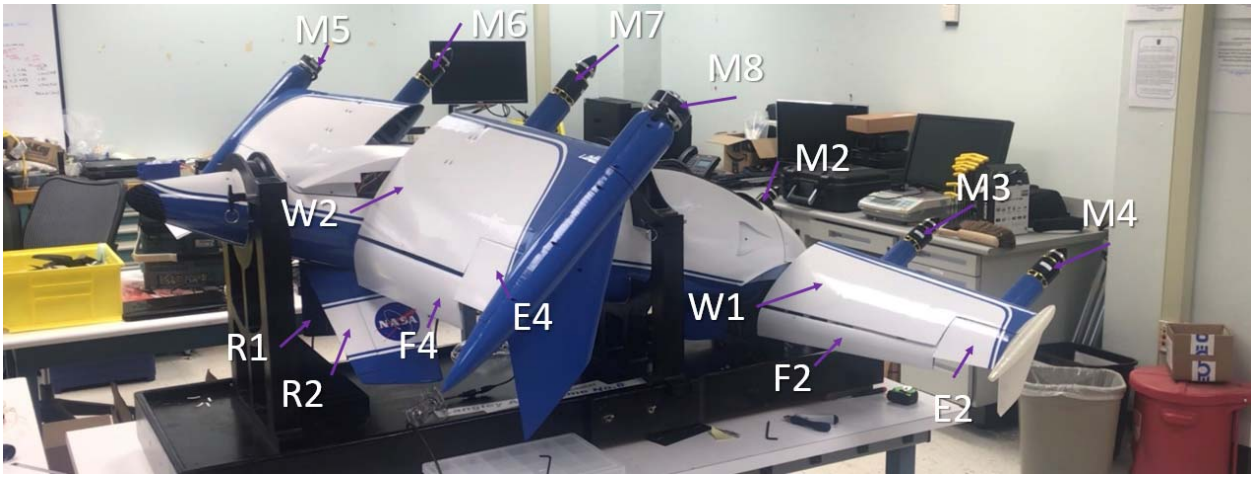

Figure 45. LA-8 Control Surface and Motor Ground Test

A load test of the entire airframe was conducted in preparation for supporting wind tunnel and flight testing. This load test was to provide verification that loading conditions planned for tunnel and flight would be supported by the airframe. The airframe was originally designed to meet 3G flight loading conditions for a 55 lb all up weight with a 1.5 safety factor. Several key structures were load tested: wing spar, wing actuator carry through, and fuselage sting mounting. Figure 46 shows how the wing load test was setup. The load distribution was based on the predicted wing loading distribution from XFLR5 for a 55 lb vehicle. The tested load case represented a 3G flight loading condition for a 65 lb all up weight. The weight placed on the model during this test was 43.75 lb per half span wing (175 lb Total). No visual or audible structural failures were observed during the load test. The 65 lb all up weight was based on accounting for the model weight to exceed the designed target takeoff weight.

Figure 46. LA-8 65lb 3G Load Test

After the control surface and load test was completed, it was time to thermally test the electrical power system. Four major components were to be tested, these included: Schottky Diodes, Electronic Speed Controllers, Battery Leads and Cooling Fans. The initial design included internally mounted cooling fans to cool the ESC's because they were located inside the fuselage and have no access to external air cooling. The fans were selected to blow air from the side air intakes directly over the top of the ESC's. Temperatures were measured using a combination of thermal images, thermocouples, and internal ESC temperature sensors. The vehicle was held to the ground using a custom stand and sandbags shown in Figure 47. Three power conditions were tested to include low (7 lb/motor), medium (8 lb/ motor) and high (9 lb/ motor) power. To account for the uncertainty in the final take-off weight, 65 lb was assumed to represent hover thrust requirements to include control authority margins.

Figure 47. LA-8 Secured During Thermal Testing

During the high power testing, temperatures were observed in Figure 48 to exceed the rated Schottky Diode component temperatures of 126 degrees Celsius before steady state temperatures were reached. This led to the decision to remove them from the system because adequate cooling was not provided, and the battery failure mode was not a concern during near term upcoming scheduled wind tunnel testing. After the Schottky Diodes were removed additional testing was conducted looking at the ESC's. Utilizing medium power settings with no cooling fans, a temperature of 106 degrees Celsius steady state was observed in Figure 49. It was desired to operate below 90 degrees Celsius, so cooling fans were required to reduce temperatures for steady state, long duration operation. A comparison with the internal temperature sensor shown in Figure 50 and the thermal image indicated an 18 degree Celsius difference. Because the thermal images provided a calibrated temperature measurement, the difference was used for future reference of the internal ESC temperature measurement with the fuselage closed and no ability to collect thermal images.

Figure 48. Diode Test Abort Temperature @ 72lb Total Thrust

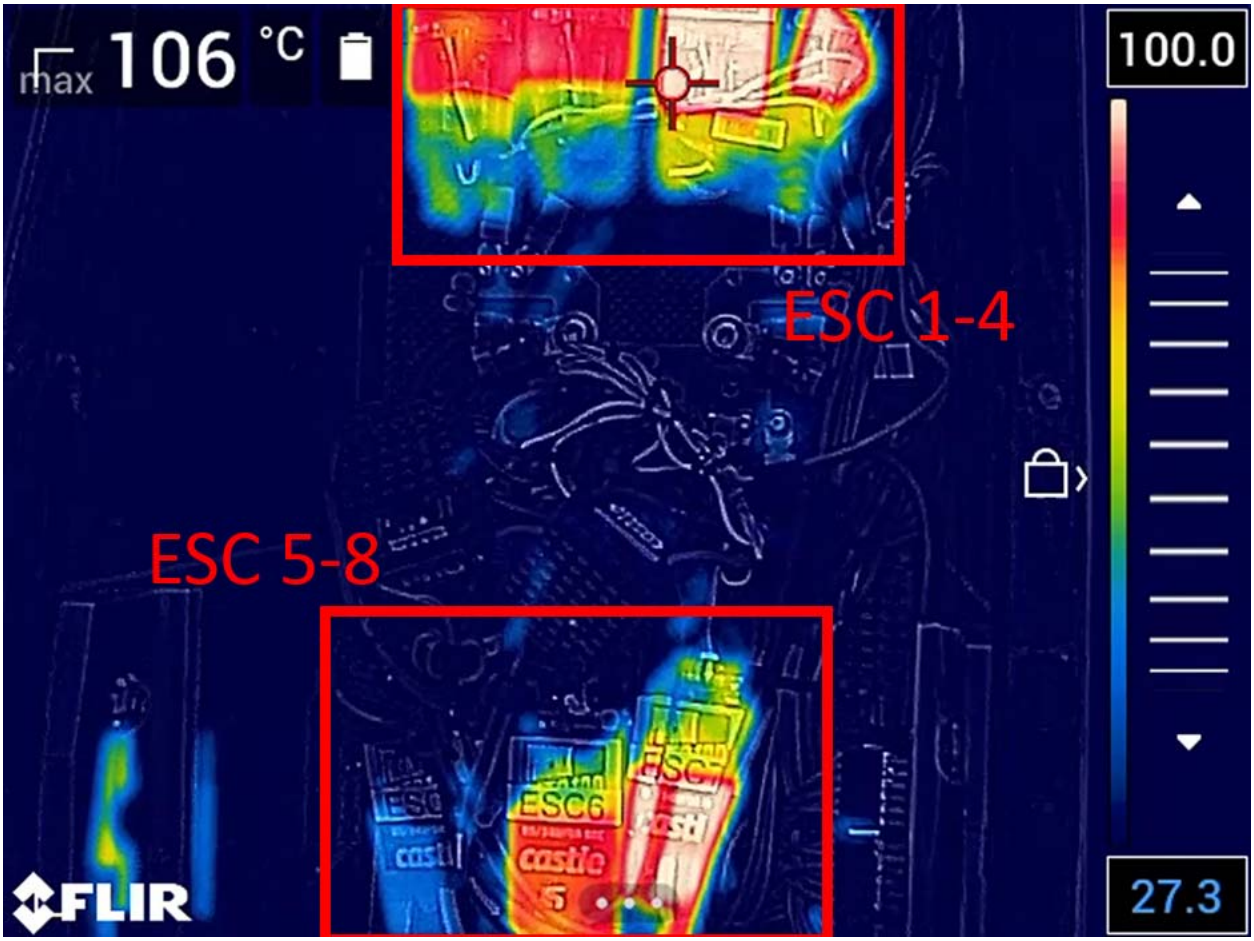

Figure 49. Steady State ESC Temperature @ 64lb Total System Thrust

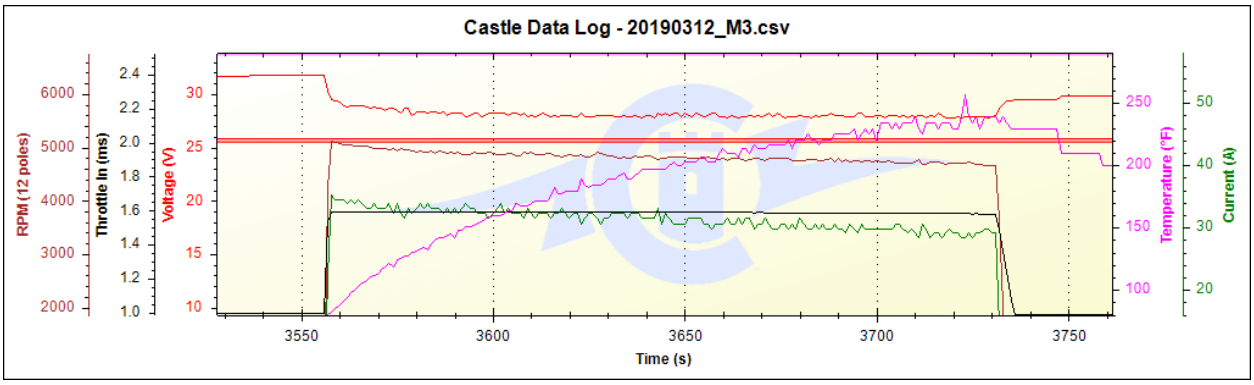

Figure 50. Internal ESC Temperature @ 64lb Total System Thrust

The final thermal test prior to wind tunnel testing was conducted running hover thrust settings (8 lb/propeller) for 10 minutes as shown in Figure 51. This provided an indication of steady state temperatures that could be expected during long duration tunnel or flight testing. Based on testing it was concluded that with the current configuration the vehicle could be operated for long duration periods at a hover thrust condition and would see external ESC temperatures of 120 degrees Celsius. Although this temperature was higher than desired, it was under the ESC internal temperature alarm (143C/290F). It was concluded that the risk of an ESC over temperature during wind tunnel testing was low, therefore no configuration changes were required to support wind tunnel testing. A thermal image of the motors in Figure 52 was also taken to provide a reference for the motor external temperatures.

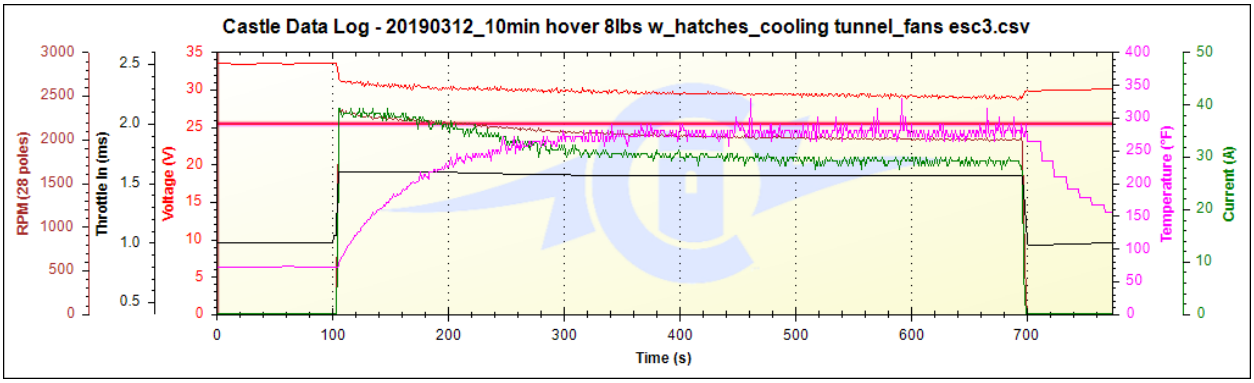

Figure 51. ESC Temperature @ 64lb Total System Thrust w/Cooling Fans

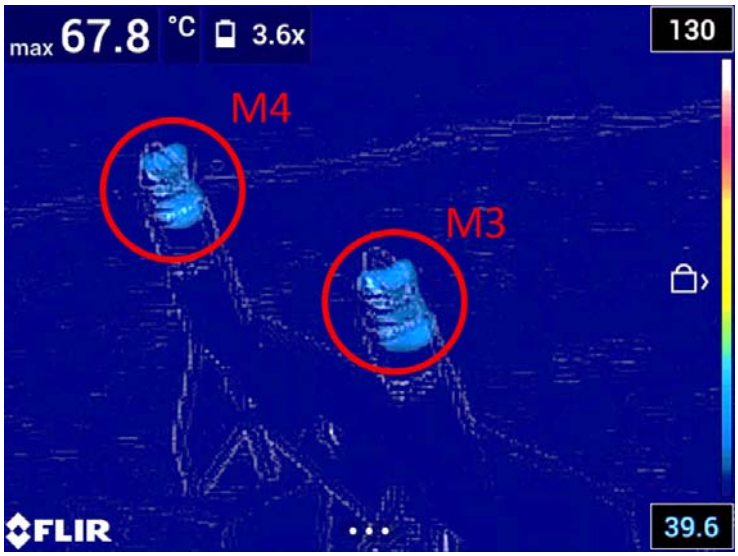

Figure 52. Steady State Motor Temperature @ 64lb Total System Thrust

Conclusions and Lessons Learned

Over the course of a year, a modular aerodynamic testbed was designed, built, and ground tested to prove out the RapidPACT process. Development of the RapidPACT process leveraged low cost electronics, additive manufactuered parts, and an agile project management approach. The following describes some lessons learned associated with this work.

The project was an incubation effort, which encouraged the project scope to grow over the course of the year. This meant the team had to grow to accomplish the larger project goals. With a focus on rapid development, it is critical to have all members engaged full time. This also needs to be paired with all team members trying to prevent scope creep.

Since the project needed large additive manufactured parts for the test model, it was important to design the parts as multiple smaller parts vs. a single large part. Even if there is capability to print large parts, there is a higher risk to the project schedule if the single large printed part fails quality assurance tests. To mitigate this risk to project schedule, the team targeted maximum build times of 48 hours per part to help reduce schedule slips on the project.

The complex geometries on parts provided a challenge for removing the support structures that are printed with the parts. Nylon parts had a risk to deform when dissolving support structure. Securing the part in the bath and carefully setting and monitoring the bath temperature mitigated this risk.

With a desire to generate aerodynamic data from the testbed, there was consideration for the surface finish on the additive manufactured parts. The nylon material generally required sanding to meet surface quality expectations, which should be accounted for by increasing labor cost of the part.

For the electronics system safety, the importance of the remote control multiplexer switch signal was proven during ground testing. When dealing with high power or high speed system components the need for a well understood non-research control system is required.

With the need for a lot of electrical signal harnesses, the flexibility of the wire became very important. Very stiff wiring for harnesses was used initially but caused concern for damaging electrical connections while working in the fuselage. Very flexible wire was used to mitigate the risk of wires causing damage to electrical connections while working inside the fuselage.

Wind-tunnel and flight testing are planned to address risks identified in the design process and will be published when data are available.

Future Work

As of September 2019, LA-8 has completed two wind tunnel tests. Future reports covering these tests are expected. Flight testing is planned for Q1 of FY2020. Wind tunnel data will be used to develop aerodynamic models of LA-8. This data will also enable flight testing either through flight control development or flight controller integration. The data will also enable comparison with predictions obtained through conceptual design tools. The main vehicle operation mode of interest is transition, since this is the condition that is more difficult to predict with low fidelity design and analysis tools.

References

1. Hiem, Eugene; Viken, Erik; Brandon, Jay; and Croom, Mark: *NASA's Learn-to-Fly Project Overview.* AIAA Aviation and Aeronautics Forum (Aviation 2018). Atlanta, GA. 2018. https://ntrs.nasa.gov/archive/nasa/casi.ntrs.nasa.gov/20190027218.pdf
2. McSwain, Robert; Glaab, Louis; and Theodore, Colin: *Greased Lightning (GL-10) Performance Flight Research – Flight Data Report.* NASA/TM–2017-219794. https://ntrs.nasa.gov/archive/nasa/casi.ntrs.nasa.gov/20180000765.pdf
3. Ambysoft: *Examining the Agile Manifesto*. http://www.ambysoft.com/essays/agileManifesto.html
4. *V/STOL Aircraft and Propulsion Concepts*. https://vertipedia-legacy.vtol.org/vstol/wheel.htm. Accessed 29 Aug 2019.
5. *OpenVSP*. http://openvsp.org/. Accessed 29 Aug 2019.
6. Antcliff, Kevin; Whiteside, Siena K. S.; Kohlman, Lee W.; and Silva, Christopher. *Baseline Assumptions and Future Research Areas for Urban Air Mobility Vehicles*. AIAA Scitech 2019 Forum. 7-11 January 2019. https://doi/abs/10.2514/6.2019-0528.
7. Patterson, James; and Bartlett, Glynn: *Effect of a Wing-Tip Mounted Pusher Turboprop on the Aerodynamic Characteristics of a Semi-Span Wing*. 21st Joint Propulsion Conference. 8-11 July, 1985. https://doi.org/10.2514/6.1985-1286.
8. Miranda, L. R. and Brennan, J. E.: *Aerodynamic Effects of Wingtip-Mounted Propellers and Turbines*. 4th Applied Aerodynamics Conference, 1986. Monterey, CA. https://doi.org/10.2514/6.1986-1802.
9. Borer, Nicholas K; Patterson, Michael D.; Viken, Jeffrey K.; Moore, Mark D.; Bevirt, JoeBen; Stoll, Alex M.; and Gibson, Andrew R.: *Design and Performance of the NASA SCEPTOR Distributed Electric Propulsion Flight Demonstrator*. 16th AIAA Aviation Technology, Integration, and Operations Conference. 13-17 June 2016. Washington, D.C. https://doi.org/10.2514/6.2016-3920.
10. Patterson, M. D.: *Conceptual Design of High-Lift Propeller Systems for Small Electric Aircraft*. Ph.D. Thesis. Georgia Institute of Technology. 2016. http://hdl.handle.net/1853/55569.
11. Gentry, Garl L., J., Takallu, M. A., and Applin, Z. T., *Aerodynamic Characteristics of a Propeller-Powered High-Lift Semispan Wing*, NASA-TM-4541, 1994.
12. Kuhn, R; Draper, J: *Investigation of Effectiveness of Large-chord Slotted Flaps in Deflecting Propeller Slipstreams Downward for Vertical Take-off and Low-speed Flight*. NACA-TN-3364, 1955. http://ntrs.nasa.gov/search.jsp?R=19930084526.
13. Viken, J.; Viken, S.; Deere, K.; Carter, M.: Design of the Cruise and Flap Airfoil for the X-57 Maxwell Distributed Electric Propulsion Aircraft. AIAA AVIATION Forum, 2017. https://doi.org/10.2514/6.2017-3922.
14. *XFLR5*. Software Package. Ver. 6.43, GNU General Public License. http://www.xflr5.com/xflr5.htm.

15. Drela, M and Youngren, H. *XFOIL: Subsonic Airfoil Development System*. Software Package. GNU General Public License. https://web.mit.edu/drela/Public/web/xfoil.
16. Feagin, Richard C. and Morrison, William D., Jr.: Delta Method, An Empirical Drag Buildup Technique. NASA-CR-151971. Dec 1, 1978. https://ntrs.nasa.gov/search.jsp?R=19790009630
17. Raymer, Daniel P.: *Aircraft Design: A Conceptual Approach*. 4th Edition. American Institute of Aeronautics and Astronautics. 2006.

REPORT DOCUMENTATION PAGE

Form Approved
OMB No. 0704-0188

1. REPORT DATE *(DD-MM-YYYY)*	2. REPORT TYPE	3. DATES COVERED *(From - To)*
1-01-2020	Technical Memorandum	

4. TITLE AND SUBTITLE

An Experimental Approach to a Rapid Propulsion and Aeronautics Concepts Testbed

5a. CONTRACT NUMBER

5b. GRANT NUMBER

5c. PROGRAM ELEMENT NUMBER

6. AUTHOR(S)

McSwain, Robert G.; Geuther, Steven C.; Howland, Gregory; Patterson, Michael D.; Whiteside, Siena K.; North, David D.

5d. PROJECT NUMBER

5e. TASK NUMBER

5f. WORK UNIT NUMBER
629660.02.30.07.01

7. PERFORMING ORGANIZATION NAME(S) AND ADDRESS(ES)

NASA Langley Research Center
Hampton, VA 23681-2199

8. PERFORMING ORGANIZATION REPORT NUMBER
L-21052

9. SPONSORING/MONITORING AGENCY NAME(S) AND ADDRESS(ES)

National Aeronautics and Space Administration
Washington, DC 20546-0001

10. SPONSOR/MONITOR'S ACRONYM(S)
NASA

11. SPONSOR/MONITOR'S REPORT NUMBER(S)
NASA-TM-2020-220437

12. DISTRIBUTION/AVAILABILITY STATEMENT

Unclassified-
Subject Category 05
Availability: NASA STI Program (757) 864-9658

13. SUPPLEMENTARY NOTES

14. ABSTRACT Modern aircraft design tools have limitations for predicting complex aerodynamic propulsion and airframe interactions. The demand for new tools and methods addressing these limitations is high based on recent DEP VTOL concepts being developed for Urban Air Mobility markets. It is proposed that low cost electronics and additive manufacturing can support the conceptual design of advanced autonomy enabled concepts, by facilitating rapid prototyping for experimentally driven design cycles. This approach has the potential to reduce complex aircraft concept development costs, minimize unique risks associated with the conceptual design, and shorten development schedule. A modular testbed was designed and built to support aeronautics and autonomy research targeting Urban Air Mobility applications utilizing complex transitioning aircraft configurations. The testbed is a modular wind tunnel and flight model. The testbed airframe is approximately 80% printed, with some minor labor required for assembly. All wind tunnel structural loading and electrical ground testing was successful. Wind tunnel testing and flight testing is planned for future work.

15. SUBJECT TERMS

3D Printed; Aircraft Design; DEP; Experimental; Flight Test; Tilt-wing; UAM; VTOL; Wind Tunnel

16. SECURITY CLASSIFICATION OF:			17. LIMITATION OF ABSTRACT	18. NUMBER OF PAGES	19a. NAME OF RESPONSIBLE PERSON
a. REPORT	b. ABSTRACT	c. THIS PAGE			STI Help Desk (email: help@sti.nasa.gov)
U	U	U	UU	63	19b. TELEPHONE NUMBER *(Include area code)* (757) 864-9658